

University of Calgary

PRISM: University of Calgary's Digital Repository

Graduate Studies

The Vault: Electronic Theses and Dissertations

2016

Modelling Water-Hydrocarbon Mutual Solubility in Multiphase Equilibrium Calculations

Yu, Hongbo

Yu, H. (2016). Modelling Water-Hydrocarbon Mutual Solubility in Multiphase Equilibrium Calculations (Unpublished master's thesis). University of Calgary, Calgary, AB.

doi:10.11575/PRISM/26966

<http://hdl.handle.net/11023/2891>

master thesis

University of Calgary graduate students retain copyright ownership and moral rights for their thesis. You may use this material in any way that is permitted by the Copyright Act or through licensing that has been assigned to the document. For uses that are not allowable under copyright legislation or licensing, you are required to seek permission.

Downloaded from PRISM: <https://prism.ucalgary.ca>

UNIVERSITY OF CALGARY

Modelling Water-Hydrocarbon Mutual Solubility in Multiphase Equilibrium Calculations

by

Hongbo Yu

A THESIS

SUBMITTED TO THE FACULTY OF GRADUATE STUDIES
IN PARTIAL FULFILMENT OF THE REQUIREMENTS FOR THE
DEGREE OF MASTER OF SCIENCE

GRADUATE PROGRAM IN CHEMICAL AND PETROLEUM ENGINEERING

CALGARY, ALBERTA

April, 2016

© Hongbo Yu 2016

Abstract

Since the 1980s, multiphase equilibrium calculations have been well developed. Usually, water is excluded from the calculations although the amount of dissolved hydrocarbons and CO₂ in water can be substantial. There are several published four-phase flash calculation methods using a single cubic EOS to model both hydrocarbon and aqueous phases, but the predicted gas solubility in water modeled from an EOS is orders of magnitude lower than experimental data.

In this thesis, a generalized multiphase flash calculation algorithm is developed to address both the multiple phase behavior of a CO₂/crude oil system and water-hydrocarbon mutual solubility simultaneously. The hydrocarbon phases are modeled with a cubic EOS, and the water phase is modelled with Henry's law constants. Our results are compared with experimental data and calculation results from commercial software to validate the algorithm in different types of equilibria.

Acknowledgements

I would like to express the deepest appreciation to my supervisor, Dr. Zhangxing (John) Chen, for his consistent support, valuable advice and guidance over the past a few years of my graduate study.

I gratefully appreciate financial support from Foundation CMG, National Science and Engineering Research Council of Canada (NSERC) and Department of Chemical and Petroleum Engineering at the University of Calgary. I would also like to thank my committee members Dr. Jalal Abedi and Dr. Nancy Chen.

My special thanks go to my parents for their encouragement and support over the years. Last but not the least, I would like to thank Yajie Cheng for her company and love.

To My Parents

Table of Contents

Abstract	ii
Acknowledgements.....	iii
Dedication	iv
Table of Contents	v
List of Tables	vii
List of Figures	viii
List of Symbols and Abbreviations.....	x
Chapter One: Introduction	1
1.1 Literature Review.....	1
1.2 Research Objectives	5
Chapter Two: Multiphase Equilibrium Calculations	7
2.1 Mathematical Formulation.....	7
2.1.1 Material Balance Equations.....	7
2.1.2 Phase Equilibrium Equations	8
2.1.3 Phase Stability Test	9
2.2 Thermodynamic Models	10
2.2.1 Equation of State	10
2.2.2 Henry's Law	13
2.3 Computational Procedure.....	17
2.3.1 Phase Stability Calculation.....	19
2.3.2 Phase-Split Calculation	21
Chapter Three: Calculation Results and Discussion.....	24
3.1 Water-containing Binary Systems.....	24

3.1.1 Water-CO ₂	24
3.1.2 Water-C ₁	25
3.1.3 Water-C ₂	30
3.1.4 Water-C ₃	33
3.2 Water-containing Multicomponent Systems	33
3.2.1 16-Component Water-CO ₂ -Oil Mixture	35
3.2.2 12-Component Water-CO ₂ -Wasson Oil Mixture	45
Chapter Four: Conclusions and Recommendations for Future Research	53
4.1 Conclusions	53
4.2 Recommendations for Future Research	54
References	55

List of Tables

Table 2-1 Reference Henry's Law constants and water interaction coefficients (Li and Nghiem, 1986)	16
Table 3-1 Component Properties for Water-CO ₂ Binary System.....	24
Table 3-2 Component Properties for Water-C ₁ Binary System.....	25
Table 3-3 Component Properties for Water-C ₂ Binary System.....	30
Table 3-4 Component Properties for the Water-C ₃ Binary System.....	33
Table 3-5 Component properties and overall composition for the sixteen-component water-CO ₂ -hydrocarbon mixture.....	37
Table 3-6 Binary interaction parameters for the sixteen-component water-CO ₂ -hydrocarbon mixture	38
Table 3-7 Predicted Phase Mole Fractions and Compositions at 94 °F and 1,100 psia for the for the 16-Component Water-CO ₂ - Oil Mixture.....	41
Table 3-8 Predicted Phase Mole Fractions and Compositions at 94 °F and 1,170 psia for the for the 16-Component Water-CO ₂ - Oil Mixture.....	42
Table 3-9 Predicted Phase Mole Fractions and Compositions at 94 °F and 1,200 psia for the for the 16-Component Water-CO ₂ - Oil Mixture.....	43
Table 3-10 Component Properties, Feed Compositions and Binary Interaction Coefficient for 12-Component Water-CO ₂ -Wasson Oil Mixture.....	46
Table 3-11 Predicted Phase Mole Fractions and Compositions at 90 °F and 1,050 psia for the for the Water-CO ₂ -Wasson Oil Mixture	50
Table 3-12 Predicted Phase Mole Fractions and Compositions at 90 °F and 1,100 psia for the for the Water-CO ₂ -Wasson Oil Mixture	51
Table 3-13 Predicted Phase Mole Fractions and Compositions at 90 °F and 1,150 psia for the for the Water-CO ₂ -Wasson Oil Mixture	52

List of Figures

Figure 2-1 Flow Chart for Multiphase Equilibrium Calculations.....	18
Figure 3-1 Predicted Water Content in the CO ₂ -rich Phase for the Water-CO ₂ Binary System from this Work.....	26
Figure 3-2 Predicted CO ₂ Solubility in the Water Phase for the Water-CO ₂ Binary System from this Work.....	26
Figure 3-3 Predicted Water Content in the CO ₂ -rich Phase for the Water-CO ₂ Binary System from a Single EOS Model.....	27
Figure 3-4 Predicted CO ₂ Solubility in the Water Phase for the Water-CO ₂ Binary System from a Single EOS Model.....	27
Figure 3-5 Predicted Water Content in the C ₁ -rich Phase for the Water-C ₁ Binary System from this Work.....	28
Figure 3-6 Predicted C ₁ Solubility in the Water Phase for the Water-C ₁ Binary System from this Work.....	29
Figure 3-7 Predicted Water Content in the C ₁ -rich Phase for the Water-C ₁ Binary System from a Single EOS Model.....	29
Figure 3-8 Predicted C ₁ Solubility in the Water Phase for the Water-C ₁ Binary System from a Single EOS Model.....	30
Figure 3-9 Predicted Water Content in the C ₂ -rich Phase for the Water-C ₂ Binary System from this Work.....	31
Figure 3-10 Predicted C ₂ Solubility in the Water Phase for the Water-C ₂ Binary System from this Work.....	31
Figure 3-11 Predicted Water Content in the C ₂ -rich Phase for the Water-C ₂ Binary System from a Single EOS Model.....	32
Figure 3-12 Predicted C ₂ Solubility in the Water Phase for the Water-C ₂ Binary System from a Single EOS Model.....	32
Figure 3-13 Predicted Water Content in the C ₃ -rich Phase for the Water-C ₃ Binary System from this Work.....	34
Figure 3-14 Predicted C ₃ Solubility in the Water Phase for the Water-C ₃ Binary System from this Work.....	34
Figure 3-15 Predicted Water Content in the C ₃ -rich Phase for the Water-C ₃ Binary System from a Single EOS Model.....	35

Figure 3-16 Predicted Phase Distribution for the 16-Component Water-CO ₂ -Oil Mixture	39
Figure 3-17 Predicted CO ₂ , N ₂ and Hydrocarbon Compositions in the Water Phase for the 16-Component Water-CO ₂ -Oil Mixture	39
Figure 3-18 Predicted Water Compositions in the Oil, Gas and Solvent-rich Liquid Phases for the 16-component Water-CO ₂ - Oil Mixture	40
Figure 3-19 Comparisons of 3-Phase Water-free and 4-Phase Water-in Equilibrium Calculations for the 16-component Water-CO ₂ -Oil Mixture.....	44
Figure 3-20 Predicted Phase Distribution for the 12-Component Water-CO ₂ -Wasson Oil Mixture.....	47
Figure 3-21 Predicted Hydrocarbon and CO ₂ Compositions in the Water Phase for the 12- Component Water-CO ₂ -Wasson Oil Mixture.....	48
Figure 3-22 Predicted Water Compositions in the Oil, Gas and CO ₂ -rich Liquid Phases for the 12-Component Water-CO ₂ -Wasson Oil Mixture.....	48
Figure 3-23 Comparisons of 3-Phase Water-free and 4-Phase Water-in Equilibrium Calculations for the 16-Component Water-CO ₂ -Wasson Oil Mixture	49

List of Symbols and Abbreviations

$a(T)$	attraction parameter in the EOS
A	equation of state parameter
b	co-volume parameter in the EOS
B	equation of state parameter
C^w	cohesive energy density of water
f_{ij}	fugacity component i in phase j
H_i	Henry's law constant of component i
H_i^*	reference Henry's law constant of component i
K_{ij}	K-value component i in phase j
N_c	number of components
N_p	number of phases
n_i	total number of moles of component i
n_{ij}	number of moles of component i in phase j
n_T	total number of moles in the system per unit bulk volume
n_j	number of moles of phase j
P	pressure
P_c	critical pressure
P_{ci}	critical pressure of component i
R	gas constant
\vec{R}	residual vector
T	temperature
T_c	critical temperature

T_{ci}	critical temperature of component i
T_F	temperature in $^{\circ}F$
T_K	temperature in K
v	molar volume
v_c	critical molar volume
v_{ci}	critical molar volume of component i
v_i^{∞}	molar volume of component i at infinite dilution
V	total volume
x_i	composition of component i
x_{ij}	composition of component i in phase j
x_{ir}	composition of component m in the reference phase
x_{it}	composition of component i in the trial phase
X_{it}	independent variables interpreted as mole number of component i
z_i	overall composition of component i
Z	compressibility factor

Greek Symbols

α_i	temperature dependent parameter of component i in the EOS
β_j	mole fraction of phase j
δ_{ik}	binary interaction parameter between components i and k
ε_{con}	convergence tolerance
$\lambda^{(k)}$	acceleration parameter
ϕ_{ij}	fugacity coefficient of component i in phase j
ω_i	acentric factor of component i

Subscripts

b	property at boiling point
c	critical property
g	gas phase
i	component index
j	phase index
k	component index
l	solvent-rich liquid phase
o	oil phase
r	reference phase
r	reduced property
w	aqueous/water phase
w	water component

Superscripts

k	iteration level
s	property at saturated state

Chapter One: **Introduction**

Multiphase equilibrium calculations have been widely used in reservoir and process simulation to determine the number of phases, phase amounts and phase compositions at a given pressure, temperature and overall compositions. Over the last few decades, multiphase flash algorithms have been well developed for different types of equilibria. In this chapter, a literature review of published research on phase equilibrium calculations and the research objectives of this thesis are presented.

1.1 Literature Review

Since Rachford and Rice (1952) published the solution of a two-phase flash calculation in 1952, many improvements have been made. Organick and Meyer (1955) presented flash calculations and results performed on an IBM card programmed calculator. Bennett et al. (1960) developed an integration method for the calculations of equilibrium flash vaporization curves. Osborne (1964) first addressed a three-phase flash problem and described a method primarily for hand calculations using a direct iteration. Deam and Maddox (1969) formulated a three-phase equilibrium problem and suggested to apply the Newton-Raphson method to solve a set of two simultaneous equations. Their three-phase flash proposal was implemented by Erbar (1972) who used the Redlich-Kwong (RK) EOS to calculate the fugacity coefficients of the vapor phase and the Scatchard-Hildebrand solubility parameter model to determine activity coefficients for the liquid phase. Dlużewski et al. (1973) developed a free-energy minimization method to calculate two- and three-phase equilibria. Lu et al. (1974) applied the RK EOS to model both the liquid and vapor phases and introduced a modified regula-falsi method to determine the compositions of two liquid phases.

An equation-of-state thermodynamic model has been extensively used to model both oil and gas phases in flash calculations since the 1970s when the Soave-Redlich-Kwong (SRK) (Soave,

1972) and Peng-Robinson (PR) (Peng and Robinson, 1976a) EOS's were developed. A typical EOS flash is formulated by material balance and the equality of component fugacity. A robust successive substitution (SS) method is commonly used to solve the fugacity equations (Prausnitz et al., 1980). A standard SS procedure contains an inner loop that performs a constant K-value flash and an outer loop that updates K-values from newly calculated component fugacities by an EOS. This method is stable; however, its convergence is very slow near critical points (Michelsen, 1982b). Fussell and Yanosik (1978) proposed a minimum variable Newton-Raphson (MVNR) iterative method to achieve quadratic convergence for a two-phase system. Fussell (1979) further generalized this MVNR method to a three-phase flash problem. The RK EOS was used in both schemes and it is applicable to all EOS's. Similar approaches can be found in Asselineau et al. (1979), Michelsen (1982b) and Abhvani and Beaumont (1987) but formulations of equations and/or different independent variables were selected. An initial guess in the vicinity of the solution is necessary for the high-order method to converge. To achieve both stability and efficiency, Mehra et al. (1983) developed an accelerated scheme of successive substitution (ACSS) that chooses an optimal step length for updating K-values in the outer loop. They reported that the number of iterations for convergence was significantly reduced by using the ACSS. Nghiem et al. (1983) combined SS and Powell's hybrid methods and developed an efficient switching criterion. Nghiem (1983) also developed a quasi-Newton successive substitution (QNSS) method that can achieve fast convergence without a good initial estimate.

Baker et al. (1982) pointed out a deficiency that an EOS can predict an incorrect number of phases and/or phase compositions by just solving a fugacity equation without incorporating the minimization of the Gibbs free energy of a system. They also presented and proved a tangent plan criterion to check if the predicted equilibrium has the global minimum Gibbs energy. On the basis

of the tangent plan criterion, Michelsen (1982a) developed a phase stability analysis algorithm that tests if the phase splitting calculation results are thermodynamically stable. The stability test results also provide an initial guess for the incipient phase compositions for the next stage phase splitting calculation if necessary. Nghiem and Li (1984) proposed a stagewise procedure using rigorous stability tests (Nghiem and Heidemann, 1982) to generate initial guesses and determined the number of phases for three-phase liquid-liquid-vapor equilibrium computations. The QNSS method (Nghiem, 1983) is applied to solve both stability test and fugacity equations. Methods that directly minimize the Gibbs free energy have also been developed and investigated by Gautam and Seider (1979), Ohanomah and Thompson (1984), Trangenstein (1985), Lucia et al. (1985), Ammar and Renon (1987), Litvak (1994) and Teh and Rangaiah (2002). However, local minimization algorithms have difficulties with existence of multiple minima while global minimization algorithms are not suitable for compositional simulation due to high computational costs (Okuno, 2009).

For water-containing systems, several authors attempted to model both hydrocarbon and water phases using a single EOS in the two- or three-phase flash calculations. Heidemann (1974) described a free-energy minimization method for three-phase flash calculations and the RK EOS was used for all phases. Peng and Robinson (1976b) used their cubic EOS (Peng and Robinson, 1976a) to predict the phase behavior of systems containing a water-rich liquid phase, a hydrocarbon-rich liquid phase and a vapor phase. Evelein et al. (1976) presented the phase behavior for CO₂/water and H₂S/water systems using a modified Redlich-Kwong EOS by Soave (Soave, 1972). In these studies, the calculated water content of the hydrocarbon phases matches well with experimental data but the dissolved gas amount in water predicted by the EOS is highly

underestimated. Modifications to the EOS parameters were also made for the aqueous phase to improve the accuracy of gas solubility calculations (Erbar et al., 1980; Peng and Robinson, 1980).

Henry's law has also been considered as a proper thermodynamic model for the aqueous phase. The following approaches used Henry's law to model the gas solubility in the aqueous phase and an EOS for the hydrocarbon phases. Luks et al. (1976) carried out calculations for air-water and nitrogen-oxygen-water systems. Heidemann and Prausnitz (1977) presented calculation results of equilibrium data for saturated combustion gases consisting of N₂, CO₂ and water. Mehra et al. (1982) used Cysewski and Prausnitz's correlation (1976) to estimate the gas solubility in the aqueous phase. Nghiem and Heidemann (1982) applied Henry's law constants obtained from experimental data in the flash calculations for crude oil/water mixtures. Li and Nghiem (1986) modified Jonah's (1983) linear correlation of Henry's law constants versus the inverse of the absolute temperature (1/T) by introducing a quadratic term of 1/T and presented the correlations for both pure water and brine obtained by regression. However, a maximum of two hydrocarbon phases was assumed in the above studies so that these models cannot predict complex multiphase behavior when satisfactory estimation of gas solubility in water is achieved.

Equilibrium calculations for four or more coexisting phases have also been proposed by several authors to address both multiple hydrocarbon phase behavior and interaction with water. Risnes and Dalen (1984) presented a stepwise procedure to perform equilibrium calculations for a four-phase liquid-liquid-vapor-water system. The approach started with a water-free two-phase flash and then additional phases were introduced and tested for existence and water was the last phase added to the system. The PR EOS was used for all phases in their calculations. Henry's law was also suggested to adjust hydrocarbon solubility to experimental data. However, no details and results were provided. Enick et al. (1986) modified the approach of Risnes and Dalen (1984) and

presented four-phase equilibrium calculations for multicomponent systems containing water. They used an alternative method to initialize the compositions of phases and a comprehensive search strategy for changes in the phase distribution before the introduction of water. The PR EOS is selected to represent both the aqueous and hydrocarbon phases. They also observed significant changes in the phase distribution occurring by introducing water. Enick et al. (1987) introduced a new mixing rule for asymmetric systems and modified EOS parameters to improve the accuracy of calculated water-CO₂ mutual solubility and water density. Wei (2015) presented a formulation of multiphase equilibrium calculations with no limit on the maximum number of phases allowed. A cubic EOS was used to calculate component fugacity and density for all phases and a phase density was corrected by a volume shift (Peneloux et al., 1982). Four-phase equilibrium calculation results were provided and changes on phase distribution under the influence of water were also observed. Both complex multiple phase behavior and interaction with the water have been addressed in the above four-phase or multiphase models. However, as discussed above, gas solubility in water calculated using an EOS is highly underestimated. Even though modifications to a mixing rule and EOS parameters were made for improvement, the reliability of predicted results is difficult to evaluate without matching experimental data.

1.2 Research Objectives

The main objective of this thesis is to develop a robust and efficient multiphase equilibrium calculation algorithm that can address both multiphase behavior and water-hydrocarbon mutual solubility simultaneously. The solid phase that can appear in asphaltic crude systems and the effect of NaCl on equilibrium are not considered in this study. To enhance the accuracy of calculation results, a cubic EOS is selected to model the hydrocarbon phases and a component fugacity in the aqueous phase is estimated by Henry's law constants. The algorithm implements a stepwise approach that sequentially applied a phase stability test and phase split calculations to determine

the correct number of phases and phase compositions. This multiphase flash routine can be used to predict and investigate complex multiphase behavior of solvent/crude oil/water mixtures and study the effect of water and dissolved gas on equilibrium results. In addition, with some modifications, it can be incorporated into a four-phase compositional simulator to investigate the effect of multiphase behavior phenomena and/or water-hydrocarbon mutual solubility on the production of gas and water-alternating-gas injection processes.

Chapter Two: Multiphase Equilibrium Calculations

In this chapter, the mathematical formulation, thermodynamic models and computational procedure for predicting multiphase equilibrium behavior are presented.

2.1 Mathematical Formulation

The mathematical formulation of a multiphase equilibrium problem is developed on the basis of material balance and the second law of thermodynamics. According to Baker et al. (1982), all phase equilibrium solutions must satisfy three restrictions:

1. Material balance
2. Equality of chemical potentials
3. Minimization of the global Gibbs energy

2.1.1 Material Balance Equations

Considering a system consisting of N_c components and N_p phases, the material balance indicates that the total mole number of a component remains the same after phase splitting. Therefore, the overall mole number of a component is equal to the sum of the mole number of that component distributed in each phase. The material balance equation on component i can be expressed as

$$n_i = \sum_{j=1}^{N_p} n_{ij} \quad (2-1)$$

where n_i is the total mole number of the i -th component and n_{ij} is the mole number of the i -th component in the j -th phase. Dividing both sides of the above equation by the total mole number of the mixture $n_T = \sum_{i=1}^{N_c} n_i$ yields

$$\frac{n_i}{n_T} = \sum_{j=1}^{N_p} \frac{n_j}{n_T} \frac{n_{ij}}{n_j} \quad (2-2)$$

Let $z_i = n_i/n_T$ denote the feed composition (overall mole fraction) of component i , $\beta_j = n_j/n_T$ denote the mole fraction of phase j , and $x_{ij} = n_i/n_{ij}$ denote the mole fraction of component i in phase j . Eqn (2-2) is written as

$$z_i = \sum_{j=1}^{N_p} \beta_j x_{ij} \quad (2-3)$$

By definition, the compositions and phase mole fractions should also satisfy

$$\sum_{i=1}^{N_c} z_i = 1 \quad (2-4)$$

$$\sum_{j=1}^{N_p} \beta_j = 1 \quad (2-5)$$

and

$$\sum_{i=1}^{N_c} x_{ij} = 1, \quad j = 1, \dots, N_p \quad (2-6)$$

2.1.2 Phase Equilibrium Equations

For an equilibrium system, the individual components have the identical chemical potentials in all the phases, which means that there is no driving force causing the components to move between the phases at equilibrium. The equality of chemical potentials can be equivalently written as

$$f_{i1}(P, T, x_{11}, \dots, x_{N_c1}) = f_{ij}(P, T, x_{1j}, \dots, x_{N_cj}), \quad j = 2, \dots, N_p \quad (2-7)$$

where $f_{ij}(P, T, x_{1j}, \dots, x_{N_cj})$ denotes the fugacity of component i in phase j at pressure P , temperature T and phase composition $(x_{1j}, \dots, x_{N_cj})$ (Firoozabadi, 2016). The component fugacity f_{ij} has the same unit as pressure and can be evaluated using

$$\ln \phi_{ij} = \ln \frac{f_{ij}}{x_{ij}P} = \int_V \left[\frac{1}{RT} \left(\frac{\partial P}{\partial n_{ij}} \right)_{T,V,\vec{n}_{ij}} - \frac{1}{V} \right] dV - \ln Z_j \quad (2-8)$$

where $\phi_{ij} = f_{ij}/(x_{ij}P)$ is the fugacity coefficient, Z_j is the compressibility factor of phase j and R is the universal constant. The partial derivatives of pressure with respect to the mole number and the integral over volume in Eqn (2-8) can be calculated according to a thermodynamic model selected.

2.1.3 Phase Stability Test

The minimization of Gibbs free energy of the system of predicted equilibrium phases is equivalent to the entropy maximum principle which is a statement of the second law of thermodynamics. As shown by Baker et al. (1982), the equality of component fugacities is necessary but not sufficient for minimization of Gibbs energy. Equilibrium that satisfies material balance and chemical potential restrictions while failing to minimize the Gibbs energy can predict an incorrect number of phases and/or phase mole fractions and compositions. Baker et al. (1982) also presented a tangent plan criterion to check if a predicted equilibrium has the global minimum Gibbs energy.

To implement the tangent plan criterion in flash calculations, Michelsen (1982a) presented a phase stability analysis method to decide whether a predicted equilibrium system is thermodynamically stable. The method introduces a trial phase to the calculated equilibrium result and tests if the Gibbs energy of the system is reduced. It examines the tangent plan distance (TPD) between the Gibbs free energy and the tangent plan at a composition $\vec{x}_t = (x_{1t}, \dots, x_{N_{ct}})$ of the trial phase. The predicted system is stable if and only if the TPD is greater than zero for all \vec{x}_t . Instead of performing an exhaustive search in the composition space, only the TPDs at stationary

points of the Gibbs free energy surface are tested. The stationary points can be located by solving the stationarity criterion equations

$$\ln X_{it} + \ln \phi_i(\vec{x}_t) - \ln x_{ij} - \ln \phi_{ij}(\vec{x}_j) = 0, \quad i = 1, \dots, N_c \quad (2-9)$$

for any phase j existing in the system, where

$$x_{it} = X_{it} / \sum_{m=1}^{n_c} X_{mt} \quad (2-10)$$

For all the non-trivial solutions \vec{X}_t of Eqn (2-9), the system of predicted equilibrium is stable if $\sum_{i=1}^{n_c} X_{it} \leq 1$. Otherwise, the system is unstable. Then a $(N_p + 1)$ -phase flash calculation is carried out to determine the corresponding phase mole fractions and compositions.

2.2 Thermodynamic Models

The reliability of the predicted phase equilibrium results highly depends on the selection of proper thermodynamic models for different phases. A cubic EOS has been widely used in the oil and gas industry for both phase behavior modelling and phase property calculations. The description of complex multiple hydrocarbon phase equilibrium by a cubic EOS is adequate enough while the gas solubility in water estimated by the same EOS is inaccurate. Therefore, in this thesis, the hydrocarbon phases are handled by a cubic EOS and the water phase is modelled by Henry's law.

2.2.1 Equation of State

An equation of state is an algebraic expression that relates the pressure, temperature and volume of a fluid phase. Among thousands of published EOS's, the cubic EOS developed by Peng and Robinson (1976a) and the Redlich-Kwong EOS modified by Soave (1972) are most commonly used in phase equilibrium calculations.

2.2.1.1 Peng-Robinson (PR) EOS

The PR EOS can be written in a pressure-explicit form as

$$P = \frac{RT}{v - b} - \frac{a(T)}{v(v + b) + b(v - b)} \quad (2-11)$$

The attraction parameter $a(T)$ and co-volume parameter b in Eqn (2-11) are calculated from the criterion of criticality

$$a(T) = 0.45724\alpha \frac{R^2 T_c^2}{P_c} \quad (2-12)$$

and

$$b = 0.0778 \frac{RT_c}{P_c} \quad (2-13)$$

with

$$\alpha = \left(1 + \lambda \left(1 - \sqrt{T/T_c}\right)\right)^2 \quad (2-14)$$

where

$$\lambda = \begin{cases} 0.37464 + 1.5432\omega - 0.26992\omega^2, & \omega < 0.49 \\ 0.3796 + 1.485\omega - 0.1644\omega^2 + 0.01666\omega^3, & \omega \geq 0.49 \end{cases} \quad (2-15)$$

ω is the acentric factor of a component that measures the non-sphericity of the molecule. For a mixture with multiple components, $a(T)$ and b are obtained from the linear mixing rules

$$a(T) = \sum_{i=1}^{n_c} \sum_{k=1}^{n_c} x_i x_k (1 - \delta_{ik}) \sqrt{a_i a_k} \quad (2-16)$$

and

$$b = \sum_{i=1}^{n_c} x_i b_i \quad (2-17)$$

where δ_{ik} is the binary interaction parameter between components i and k and for each component, a_i and b_i are computed from Eqn (2-12) and Eqn (2-13), respectively.

In terms of the compressibility $Z = PV/RT$, one may write Eqn (2-11) as

$$Z^3 - (1 - B)Z^2 + (A - 2B - 3B^2)Z - (AB - B^2 - B^3) = 0 \quad (2-18)$$

where

$$A = \frac{a(T)P}{R^2T^2} \quad (2-19)$$

and

$$B = \frac{bP}{RT} \quad (2-20)$$

Eqn (2-18) can be solved analytically by the cubic formula (Chen, 2007). If multiple real roots exist, the one giving the lowest Gibbs energy is selected (Evelein et al., 1976).

In a hydrocarbon phase, the fugacity coefficient of component i is computed by

$$\ln \phi_i = \frac{b_i}{b}(Z - 1) - \ln(Z - B) - \frac{A}{2\sqrt{2}B} \left(\frac{1}{a} \frac{\partial a}{\partial x_i} - \frac{b_i}{b} \right) \ln \left(\frac{Z + (1 + \sqrt{2})B}{Z + (1 - \sqrt{2})B} \right) \quad (2-21)$$

2.2.1.2 Soave-Redlich-Kwong (SRK) EOS

The SRK EOS can be expressed as

$$P = \frac{RT}{v - b} - \frac{a(T)}{v(v + b)} \quad (2-22)$$

Parameters $a(T)$ and b are computed from

$$a(T) = 0.42747\alpha \frac{R^2T_c^2}{P_c} \quad (2-23)$$

and

$$b = 0.08664 \frac{RT_c}{P_c} \quad (2-24)$$

with

$$\alpha = \left(1 + \lambda \left(1 - \sqrt{T/T_c}\right)\right)^2 \quad (2-14)$$

where

$$\lambda = 0.48 + 1.574\omega - 0.26992\omega^2 \quad (2-25)$$

The linear mixing rules Eqn (2-16) and Eqn (2-17) are applied to evaluate $a(T)$ and b for a mixture, with a_i and b_i for each component calculated from Eqn (2-23) and Eqn (2-24), respectively. The SRK EOS can be written as the following cubic equation in Z :

$$Z^3 - Z^2 + (A - B - B^2)Z - AB = 0 \quad (2-26)$$

where A and B are given by Eqn (2-19) and Eqn (2-20). The fugacity coefficient of component i is computed by

$$\ln \phi_i = \frac{b_i}{b} (Z - 1) - \ln(Z - B) - \frac{A}{B} \left(\frac{1}{a} \frac{\partial a}{\partial x_i} - \frac{b_i}{b} \right) \ln \left(1 + \frac{B}{Z} \right) \quad (2-27)$$

2.2.2 Henry's Law

As discussed before, the calculated phase equilibrium for a water-containing system modelled by a single EOS is not accurate in the prediction of gas in water solubility. This can be improved by applying a different but more appropriate thermodynamic model to handle the water phase during the calculation. In this work, component fugacities in the water phase is calculated using Henry's law constants correlated by Li and Nghiem (1986). The correlation was developed for a variety of components including CO₂, N₂ and hydrocarbons by performing an extensive match of experimental solubility data.

The fugacity of the water component in the water phase is calculated using the Gibbs-Duhem equation (Prausnitz, 1969)

$$f_{ww} = x_{ww} \phi_{ww}^S P_{ww}^S \exp \left(\int_{P_{ww}^S}^P \frac{v_{ww}}{RT} dP \right) \quad (2-28)$$

where w denotes the water phase and w denotes the water component.

According to Li and Nghiem (1986), the fugacity coefficient ϕ_{w}^s is determined using the following correlation in terms of temperature in $^{\circ}F$

$$\begin{aligned} \phi_{w}^s = & 0.9958 + 9.68330 \times 10^{-5}T_F - 6.715 \times 10^{-7}T_F^2 \\ & - 3.08333 \times 10^{-10}T_F^3 \quad T_F > 90 \text{ }^{\circ}F \end{aligned} \quad (2-29)$$

$$\phi_{w}^s = 1 \quad T_F \leq 90 \text{ }^{\circ}F$$

which is found by matching the data of Canjar and Manning (1967).

The saturation pressure of water P_{w}^s can be obtained by solving the Frost-Kalkwarf-Thodos vapor-pressure equation reported by Reid et al. (1977).

$$\ln P_{w}^s = B \left(\frac{1}{T_{rw}} - 1 \right) + (0.7816B + 2.67) \ln(T_{rw}) + \frac{27}{64} \left(\frac{P_{w}^s}{T_{rw}^2} - 1 \right) \quad (2-30)$$

with

$$B = \frac{\ln P_{cw} + 2.67 \ln T_{b_{rw}} + \frac{27}{64} [(1/P_{cw} T_{b_{rw}}^2) - 1]}{1 - 1/T_{b_{rw}} - 0.7816 \ln T_{b_{rw}}} \quad (2-31)$$

where T_{rw} is the reduced temperature of water, P_{cw} is the critical pressure of water and $T_{b_{rw}}$ is given by

$$T_{b_{rw}} = \frac{T_{bw}}{T_{cw}} \quad (2-32)$$

where T_{cw} is the critical temperature of water and T_{bw} is the normal boiling point.

The molar volume v_w in Eqn (2-28) is calculated from the analytical relation reported by Rowe and Chou (1970)

$$v_w = A(T_K) - B(T_K)P - C(T_K)P^2 \quad (2-33)$$

where v_w is in $cm^3/gram$, T_K is in K and P is in kgf/cm^2 . $A(T_K)$, $B(T_K)$ and $C(T_K)$ are determined as follows:

$$A(T_K) = 5.916365 - 1.035794 \times 10^{-2}T_K + 9.270048 \times 10^{-6}T_K^2 - \frac{1127.522}{T_K} + \frac{100674.1}{T_K^2} \quad (2-34)$$

$$B(T_K) = 5.204914 \times 10^{-3} - 1.0482101 \times 10^{-5}T_K + 8.328532 \times 10^{-9}T_K^2 - \frac{1.1702939}{T_K} + \frac{102.2783}{T_K^2} \quad (2-35)$$

$$C(T_K) = 1.18547 \times 10^{-8} - 6.599143 \times 10^{-11}T_K \quad (2-36)$$

The fugacity of a non-water component in the water phase modeled by Henry's law is given by

$$f_{iw} = x_{iw}H_i, \quad i \neq w \quad (2-37)$$

H_i is Henry's law constant of component i and it can be evaluated from

$$\ln H_i = \ln H_i^* + \frac{v_i^\infty P}{RT} \quad (2-38)$$

In Eqn (2-38), v_i^∞ , the molar volume of component i at infinite dilution, is computed from the correlation of Lyckman et al. (1965)

$$\frac{P_{ci}v_i^\infty}{RT_{ci}} = 0.095 + 2.35 \frac{TP_{ci}}{C^w T_{ci}} \quad (2-39)$$

C^w is the cohesive energy density of water determined by

$$C^w = \frac{h_w^0 - h_w^s + P_w^s v_w^s - RT}{v_w^s} \quad (2-40)$$

where P_w^s is obtained from Eqn (2-30), v_w^s , the molar volume of water at P_w^s and T , is calculated using Eqn (2-33), and $h_w^0 - h_w^s$, the enthalpy departure of water liquid at P_w^s and T , is computed from the following Yen-Alexander equation (1965):

$$\frac{h_w^0 - h_w^s}{T_{cwK}} = \frac{7.0 + 4.5688(-\ln P_{rw})^{0.333}}{1.0 + 0.004(\ln P_{rw})} \quad (2-41)$$

P_{rw} is the reduced pressure of water and T_{cwK} is the critical temperature of water in K.

Table 2-1 Reference Henry's Law constants and water interaction coefficients (Li and Nghiem, 1986)

Component	A	B	C	δ_{iw}
C ₁	10.9554	11.3569	1.17105	0.4907
C ₂	13.9485	13.8254	1.66544	0.4911
C ₃	14.6331	14.4872	1.78068	0.5469
n-C ₄	13.4248	13.8865	1.71879	0.5080
n-C ₅	16.0045	16.2281	2.13123	0.5
n-C ₁₀	31.9431	28.6725	4.37707	0.45
N ₂	10.7090	11.4793	1.16549	0.275
CO	10.7069	11.1313	1.0892	0.2
CO ₂	11.3021	10.6030	1.20696	0.2 $T \leq 273K$ 0.49852-0.008T $T > 272K$

H_i^* is the reference Henry's law constant that can be evaluated using the following correlation suggested by Li and Nghiem (1986):

$$\ln \left(\frac{H_i^*}{f_w^S} \right) = -A + B \left(\frac{10^3}{T_K} \right) - C \left(\frac{10^6}{T_K^2} \right) \quad (2-42)$$

f_w^S , the fugacity of saturated water, is given by

$$f_w^S = \phi_w^S P_w^S \quad (2-43)$$

where ϕ_{iw}^s and P_{iw}^s are computed from Eqn (2-29) and Eqn (2-30), respectively. Coefficients A , B and C as well as the Peng-Roinson EOS binary interaction parameters with water δ_{iw} for various components were obtained by regression and provided in Table 2-1.

2.3 Computational Procedure

A stepwise method that sequentially applies the phase stability test and phase split calculations is used to compute the phase equilibrium results. The calculation is started by performing a stability test for the feed phase. If the feed phase is stable, the calculation is done and the system only contains a single phase. Otherwise, another phase is introduced into the system and the phase-split calculation is carried out to obtain the mole fraction and composition of each phase. Then one of the phases is selected to be tested for stability and phase-split calculations are performed if necessary. The procedure repeats until the entire multiphase system is thermodynamically stable or the maximum allowable number of phases is achieved. The computational flow chart is shown in Fig. 2-1.

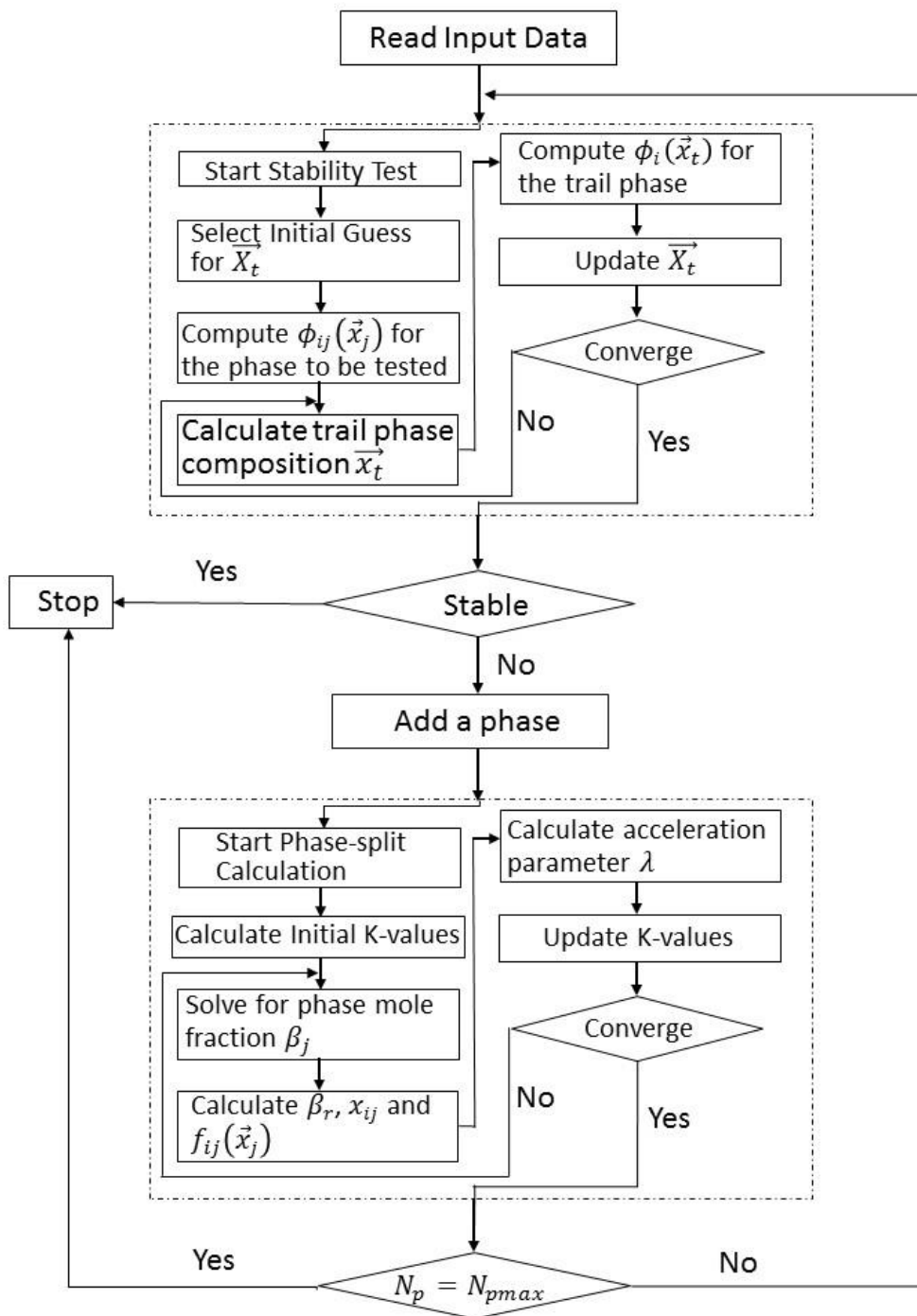


Figure 2-1 Flow Chart for Multiphase Equilibrium Calculations

2.3.1 Phase Stability Calculation

The stability of a multiphase system can be investigated by solving Eqn (2-9):

$$\ln X_{it} + \ln \phi_i(\vec{x}_t) - \ln x_{ij} - \ln \phi_{ij}(\vec{x}_j) = 0, \quad i = 1, \dots, N_c \quad (2-9)$$

where j denotes one of the phases existing in the current equilibrium system. A successive substitution iteration (SSI) is used to find the solution. During iteration, \vec{X}_t is updated by

$$X_{it}^{(k+1)} = \exp\left(\ln x_{ij} + \ln \phi_{ij}(\vec{x}_j) - \ln \phi_i(\vec{x}_t^{(k)})\right), \quad i = 1, \dots, N_c \quad (2-44)$$

where superscript (k) denotes the iteration level. The fugacity coefficients $\phi_{ij}(\vec{x}_j)$ and $\phi_i(\vec{x}_t^{(k)})$ are calculated from an EOS for a hydrocarbon phase or from Henry's law constants for the water liquid phase. The phase is identified as water only if the water component composition in the phase is greater than 0.8 and the system pressure is greater than the estimated water vapor pressure calculated from Eqn (2-30).

Several initial guesses for \vec{X}_t were suggested by Li and Firoozabadi (2012) to effectively locate the stationary points of the Gibbs free energy and the following order applies:

- 1) The Wilson correlation (Wilson, 1969)

$$X_{it}^{(0)} = z_i K_i^{wilson}, \quad i = 1, \dots, N_c \quad (2-45)$$

where

$$K_i^{wilson} = \frac{P_{ci}}{P} \exp\left(5.37(1 + \omega_i) \left(1 - \frac{T_{ci}}{T}\right)\right) \quad (2-46)$$

- 2) The inverse Wilson correlation

$$X_{it}^{(0)} = z_i / K_i^{wilson}, \quad i = 1, \dots, N_c \quad (2-47)$$

- 3) The cubic root of the Wilson correlation

$$X_{it}^{(0)} = z_i \sqrt[3]{K_i^{Wilson}}, \quad i = 1, \dots, N_c \quad (2-48)$$

4) The inverse cubic root of the Wilson correlation

$$X_{it}^{(0)} = z_i / \sqrt[3]{K_i^{Wilson}}, \quad i = 1, \dots, N_c \quad (2-49)$$

5) A pure species

$$X_{it}^{(0)} = 0.9 \quad \text{and} \quad X_{kt}^{(0)} = \frac{0.1}{N_c - 1} \quad \text{for } i = 1, \dots, N_c \text{ and } k \neq i \quad (2-50)$$

The details of the algorithm for phase stability calculations using SSI are as follows:

1. Obtain an initial guess for \vec{X}_t from Eqns (2-45) to (2-50)
2. Compute the fugacity coefficient $\phi_{ij}(\vec{x}_j)$ for the phase to be investigated for stability using
 - 2.1. Eqn (2-21) or Eqn (2-27) according to the EOS selected for a hydrocarbon phase
or
 - 2.2. Eqn (2-28) and Eqn (2-37) for the water phase
3. Calculate the trial phase composition \vec{x}_t from Eqn (2-10)
4. Calculate the fugacity coefficient $\phi_i(\vec{x}_t)$ for the trial phase similarly as in Step 2
5. Update $X_{it}^{(k+1)}$ from Eqn (2-44) and check for convergence by satisfying

$$\left\| \vec{X}_t^{(k+1)} - \vec{X}_t^{(k)} \right\| < \varepsilon_{con}$$

6. If it does not converge, go to Step 3. If the convergence has been achieved, check phase stability using

$$\sum_{i=1}^{N_c} X_{it} \leq 1$$

7. If the above inequality holds, the system is stable. Go to step 1 and perform another stability test calculations using a different initial guess. Otherwise, the system is not stable, and then start the next stage phase-split calculations with a newly introduced phase.

2.3.2 Phase-Split Calculation

If an unstable system is detected, a phase-split calculation with an additional phase is then carried out to determine the mole fraction and composition of each phase. An acceleration scheme of the successive substitution iteration (ACSSI) is used in the phase-split calculations. To implement ACSSI, it is more convenient to work with K-values which are the ratios of the composition of component i in phase j to those in a reference phase:

$$K_{ij} = \frac{x_{ij}}{x_{ir}} \quad i = 1, \dots, N_c \text{ and } j = 1, \dots, N_p \quad (2-51)$$

Therefore, the material balance equations can be written as

$$z_i = \sum_{p=1}^{N_p} \beta_p K_{ip} x_{ir} \quad i = 1, \dots, N_c \quad (2-52)$$

and x_{ij} , β_j and z_i are related by the following equation:

$$x_{ij} = \frac{K_{ij} z_i}{\sum_{p=1}^{N_p} \beta_p K_{ip}} \quad i = 1, \dots, N_c \quad (2-53)$$

The mole fraction of the reference phase can be eliminated using Eqn (2-5) and $K_{ir} = 1$ by definition. Substitution of Eqn (2-53) into the constraint equations Eqn (2-6) on phase composition gives the multiphase Rachford-Rice equations

$$\sum_{i=1}^{N_c} \frac{(K_{ij} - 1) z_i}{1 + \sum_{p=1, p \neq r}^{N_p} \beta_p (K_{ip} - 1)} = 0 \quad j = 1, \dots, N_p \text{ and } j \neq r \quad (2-54)$$

Eqn (2-54) can be solved for β_p by the Newton-Raphson method with the Jacobian elements evaluated by

$$a_{mn} = - \sum_{i=1}^{N_c} \frac{(K_{im} - 1)(K_{in} - 1)z_i}{\left(1 + \sum_{p=1, p \neq r}^{N_p} \beta_p (K_{ip} - 1)\right)^2} \quad (2-55)$$

After β_j 's are obtained, β_r can be directly calculated from Eqn (2-5) and phase compositions x_{ij} are computed using Eqn (2-53). The component fugacity coefficients $f_{ij}(\vec{x}_j)$ are obtained according to the phase type and corresponding thermodynamic models. Eqn (2-21) or Eqn (2-27) is used for the hydrocarbon phases and Eqn (2-28) and Eqn (2-37) are used for the water phase. The K-values are updated using an acceleration scheme developed by Mehra et al. (1983) for fast convergence. The acceleration parameter $\lambda^{(k+1)}$ is calculated by the following equation:

$$\lambda^{(k+1)} = \frac{\lambda^{(k)} \sum_{i=1}^{N_c} \sum_{j \neq r}^{N_p} (g_{ij}^{(k)})^2}{\left| \sum_{i=1}^{N_c} \sum_{j \neq r}^{N_p} \left((g_{ij}^{(k-1)} g_{ij}^{(k)}) - (g_{ij}^{(k)})^2 \right) \right|^2}, \quad i = 1, \dots, N_c \quad (2-56)$$

where the superscript (k) is the iteration level and

$$g_{ij} = \ln \frac{f_{ir}}{f_{ij}}, \quad i = 1, \dots, N_c \quad (2-57)$$

$\lambda^{(k+1)}$ is initialized with 1 and limited within the range [1,3]. Then the K-values are updated from

$$K_{ij}^{(k+1)} = K_{ij}^{(k)} \exp\left(-\lambda^{(k+1)} \frac{f_{ij}}{f_{ir}}\right) \quad i = 1, \dots, N_c \text{ and } j \neq r \quad (2-58)$$

The initial K-values for the newly introduced phase to start the ACSSI is directly obtained from the results of a stability test:

$$K_{in_p}^{(k)} = \frac{x_{it}}{x_{ir}} \quad i = 1, \dots, N_c \quad (2-59)$$

where n_p denotes the new phase newly added to an unstable system.

The algorithm for phase-split calculations using SSI is as follows:

1. Calculate the initial K-values for the newly added phase from Eqn (2-59)
2. Solve for β_j from Eqn (2-54) using the Newton-Raphson method
3. Calculate the reference phase mole fraction β_r from Eqn (2-5)
4. Calculate the phase composition x_{ij} from Eqn (2-53)
5. Compute the component fugacity $f_{ij}(\vec{x}_j)$ for each phase using
 - 5.1 Eqn (2-21) or Eqn (2-27) according to the EOS selected for a hydrocarbon phase or
 - 5.2 Eqn (2-28) and Eqn (2-37) for the water phase
6. Calculate the acceleration parameter from Eqn (2-56)
7. Update K-values using Eqn (2-58)
8. Check for convergence by the following criterion:

$$\left[\sum_{\substack{j=1 \\ j \neq r}}^{N_p} \sum_{i=1}^{N_c} (f_{ij} - f_{ir})^2 \right]^{\frac{1}{2}} < \varepsilon_{con}$$

9. If the convergence has been achieved, select a reference phase and perform the stability as described in Section 2.3.1. Otherwise, go to Step 2 to continue ACSSI.

Chapter Three: Calculation Results and Discussion

This chapter presents results of multiphase equilibrium calculations for both binary and multicomponent water-containing systems. Up to four phases (oil, gas, solvent-rich liquid and water) are found coexisting at equilibrium in the systems to be investigated. The predicted equilibrium results are compared to experimental data and those obtained from commercial software to verify the accuracy and robustness of our algorithm in the prediction of different types of equilibria. Results calculated using a single EOS for all the phases are also presented to demonstrate the effectiveness of Henry's law in modeling gas solubility. In addition, the effect of water on multiple hydrocarbon phase behavior is also studied.

The chart legends presented in this chapter have the following meaning:

- ‘_EXP’ denotes experimental data
- ‘_CAL’ denotes the results calculated from our algorithm
- ‘_EOS’ denotes the results calculated from a single EOS model for all phases

3.1 Water-containing Binary Systems

The calculated compositions of the water component in the gas/oil phases and solutes in the water phase for various binary systems are presented. The PR EOS is used to compute the component fugacity of the gas phase and the water phase is modeled by Henry's law. The binary interaction parameter is obtained from Li and Nghiem (1986) as listed in Table 2-1. Henry's law constants adopted in our algorithm give a satisfactory match with experimental data as expected since they were correlated through regressions (Li and Nghiem, 1986). In contrast, the amounts of dissolved hydrocarbons and CO₂ in the water phase calculated from a single EOS model that uses the PR EOS for both phases differ by orders of magnitude compared with laboratory measurements.

3.1.1 Water-CO₂

Table 3-1 Component Properties for Water-CO₂ Binary System

Component	P_c (psia)	T_c (°F)	v_c (ft ³ /lb-mol)	MW	ω
CO ₂	1143.345	87.89	1.505	44.01	0.225
H ₂ O	3197.838	705.47	0.897	18.015	0.344

Phase equilibria of a water-CO₂ binary system are calculated at temperature from 77 °F to 212 °F and pressure from 60 psia to 10,060 psia. Component properties used in the calculation are listed in Table 3-1 and the experimental data are taken from Wiebe (1941). As shown in Figures 3-1 and 3-2, the predicted water composition in the CO₂-rich phase matches well with the experimental data and the predicted CO₂ solubility in water is accurate except for 87.872°F at which the predicted CO₂ composition is 10 percent higher than the experimental values for pressures greater than 1000 psia. The overall accuracy of the predicted water-CO₂ mutual solubility is satisfactory.

The results calculated using a single EOS model for both phases are depicted in Figures 3-3 and 3-4. They show that the predicted water content in the CO₂-rich phase is as accurate as that obtained from this work while the predicted CO₂ solutes in water is 10 to 100 times lower than experimental data.

3.1.2 Water-C₁

Table 3-2 Component Properties for Water-C₁ Binary System

Component	P_c (psia)	T_c (°F)	v_c (ft ³ /lb-mol)	MW	ω
C ₁	667.196	-116.59	1.586	16.043	0.008
H ₂ O	3197.838	705.47	0.897	18.015	0.344

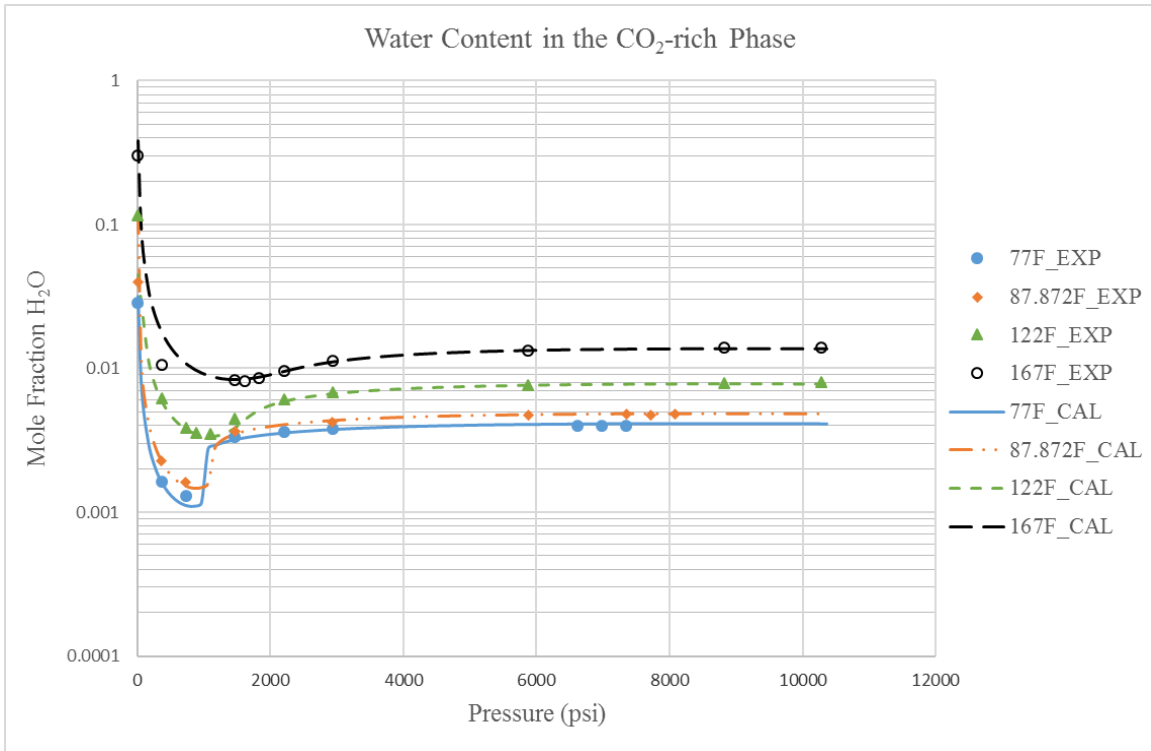


Figure 3-1 Predicted Water Content in the CO₂-rich Phase for the Water-CO₂ Binary System from this Work

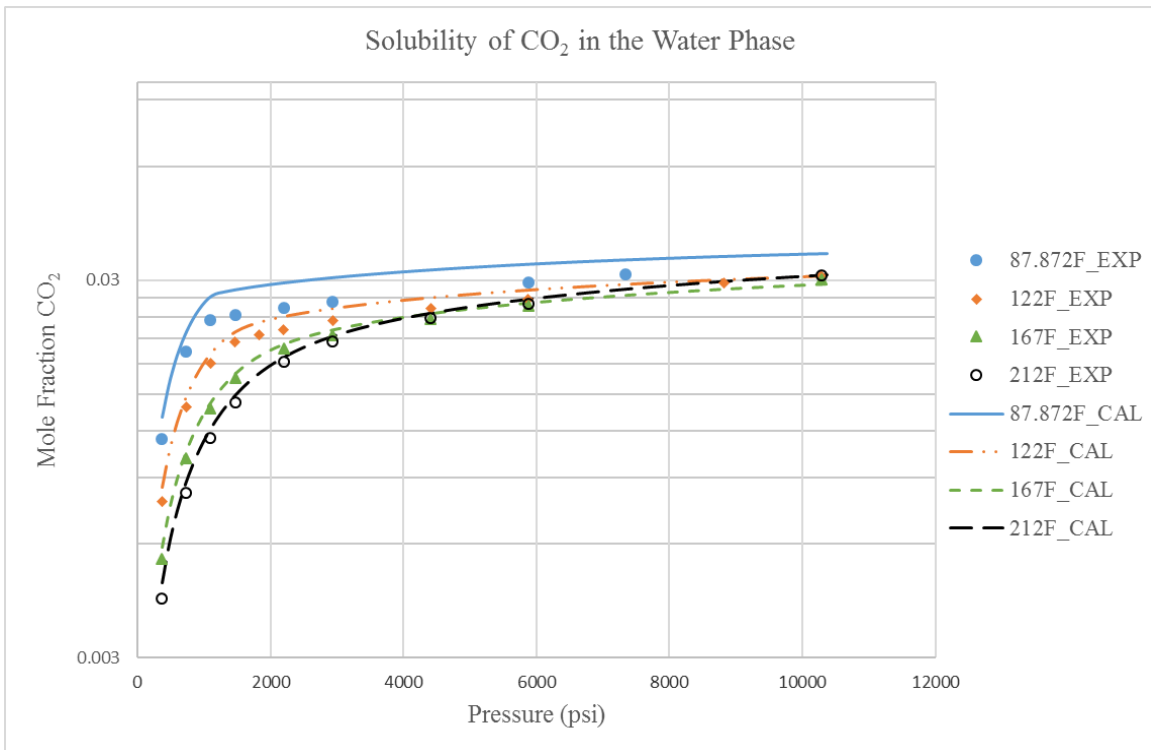


Figure 3-2 Predicted CO₂ Solubility in the Water Phase for the Water-CO₂ Binary System from this Work

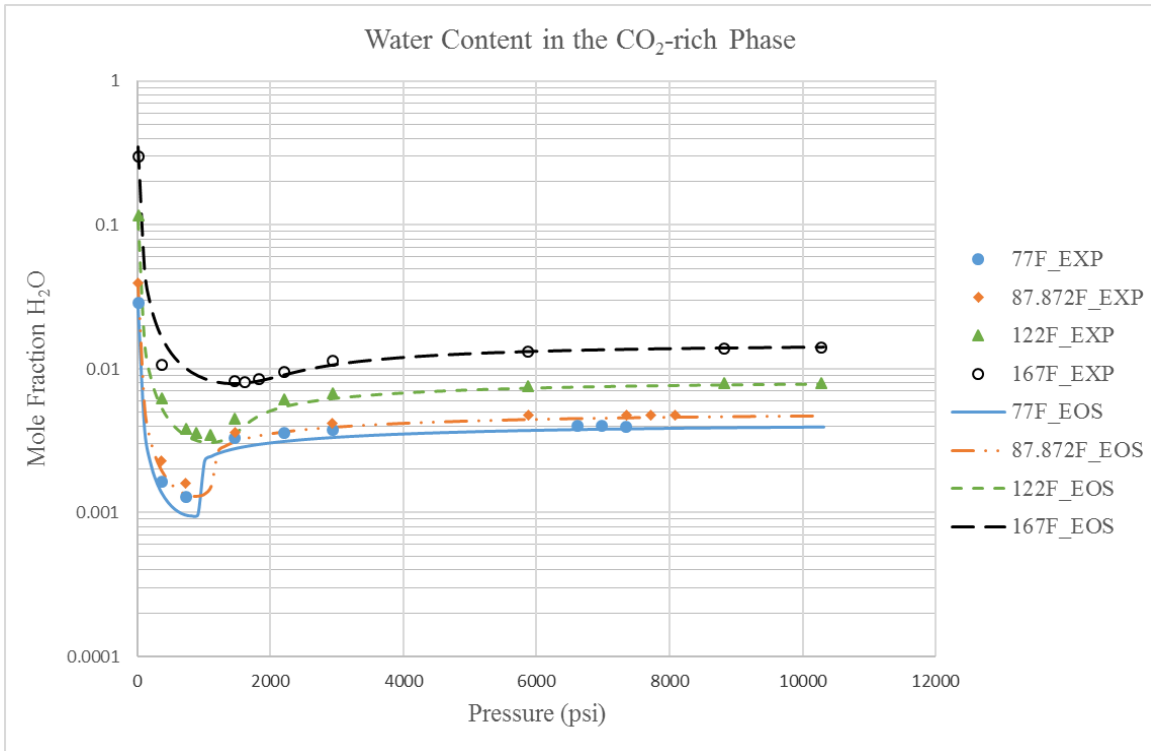


Figure 3-3 Predicted Water Content in the CO₂-rich Phase for the Water-CO₂ Binary System from a Single EOS Model

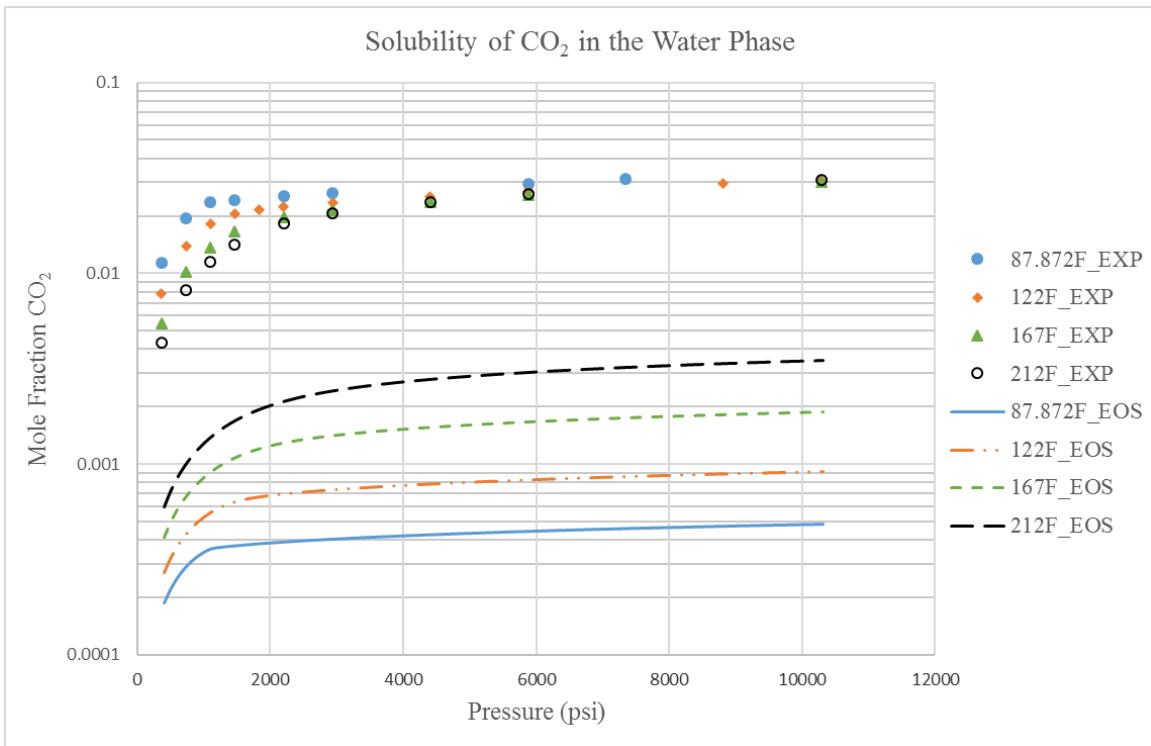


Figure 3-4 Predicted CO₂ Solubility in the Water Phase for the Water-CO₂ Binary System from a Single EOS Model

For a water-C₁ binary system, component properties are given in Table 3-2. Phase equilibrium calculations are carried out at temperature from 77 °F to 460 °F and pressure from 300 psia to 10,000 psia. The experimental data of Olds et al. (1942) for the C₁-rich phase and of Culbertson and McKetta (1951) for the water phase are compared with calculated compositions in Figures 3-5 and 3-6, and an excellent match is achieved. In contrast, a single EOS model is not able to provide accurate prediction for both water-in-C₁ and C₁-in-water compositions. As shown in Figure 3-7, the calculated water content in C₁-rich phase matches well with experimental data at 100°F but the error becomes large as temperature increases. On the other hand, from Figure 3-8, we see that the C₁ solubility in water obtained from a single EOS model is 1 to 4 orders of magnitude lower.

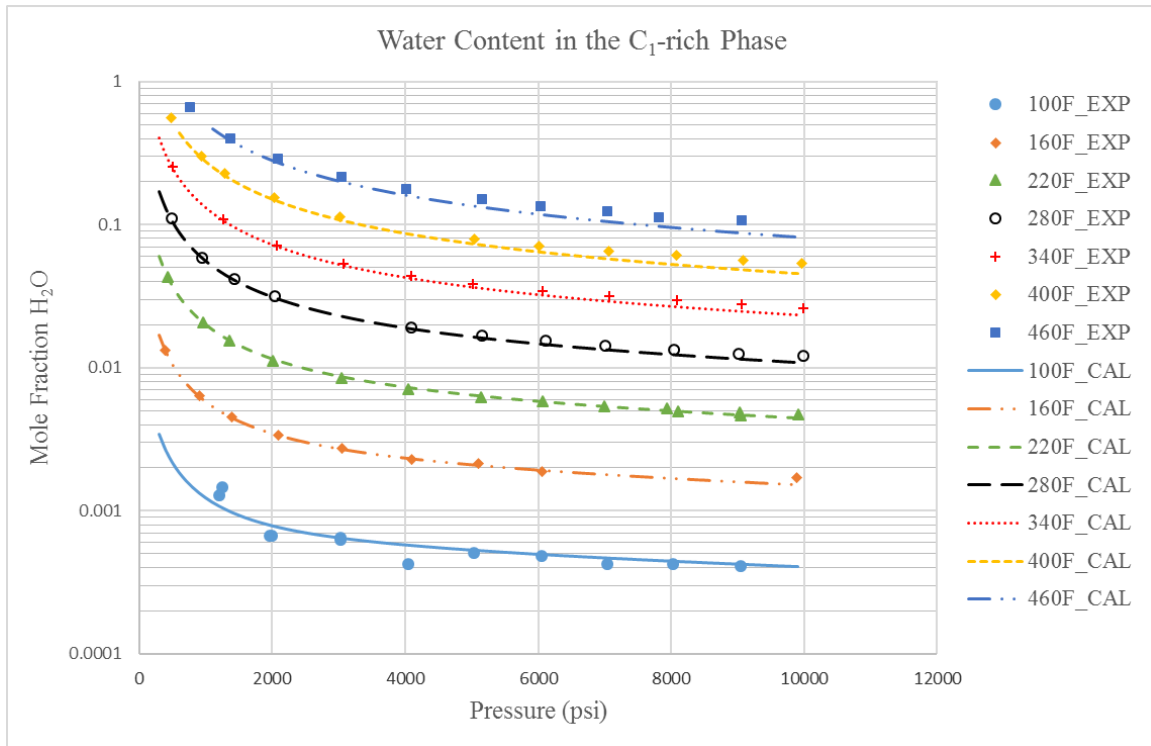


Figure 3-5 Predicted Water Content in the C₁-rich Phase for the Water-C₁ Binary System from this Work

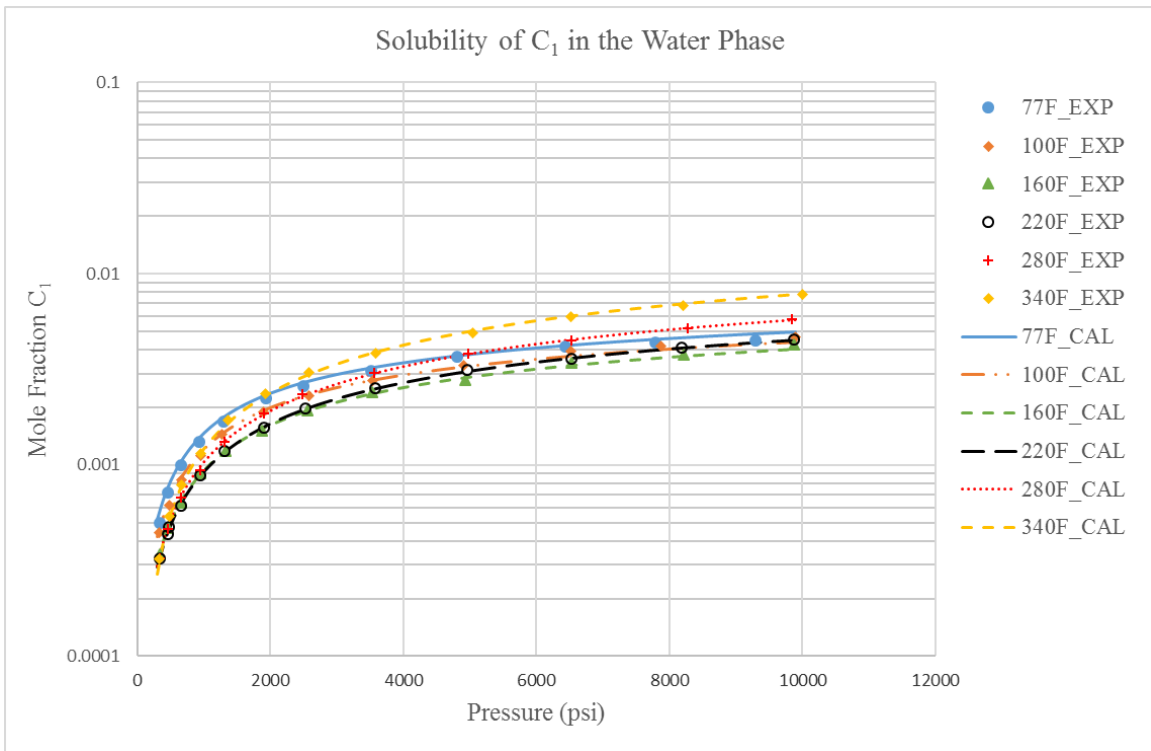


Figure 3-6 Predicted C_1 Solubility in the Water Phase for the Water- C_1 Binary System from this Work

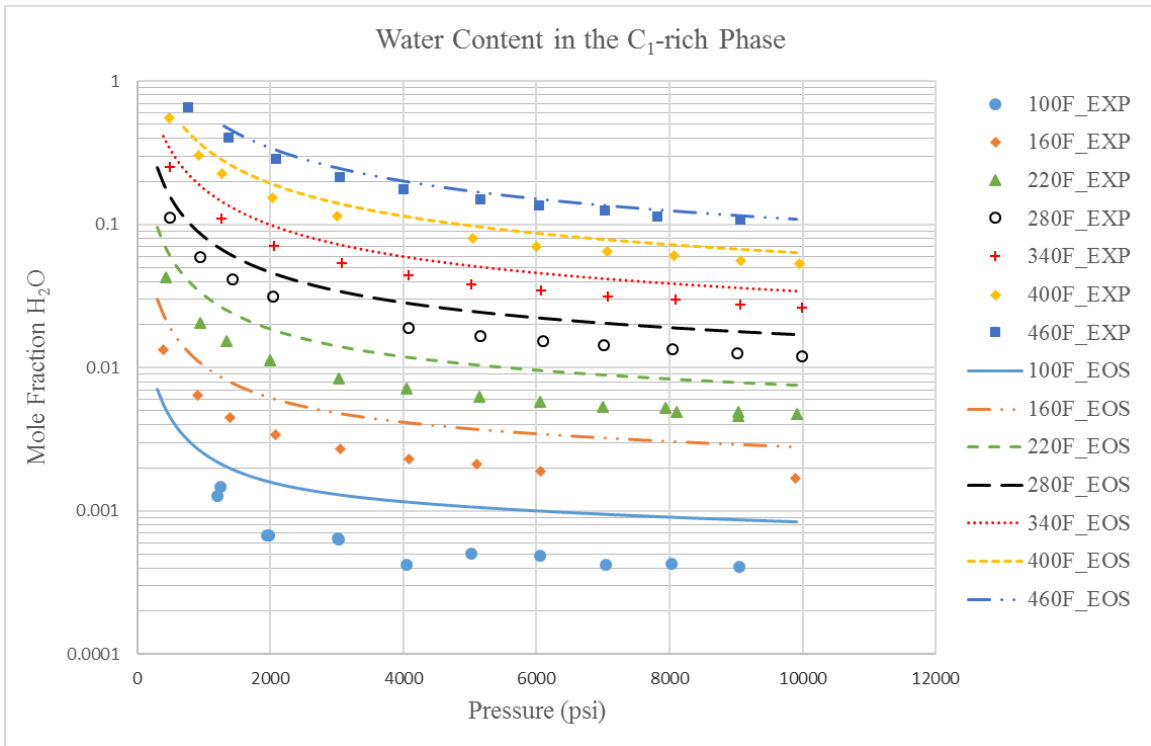


Figure 3-7 Predicted Water Content in the C_1 -rich Phase for the Water- C_1 Binary System from a Single EOS Model

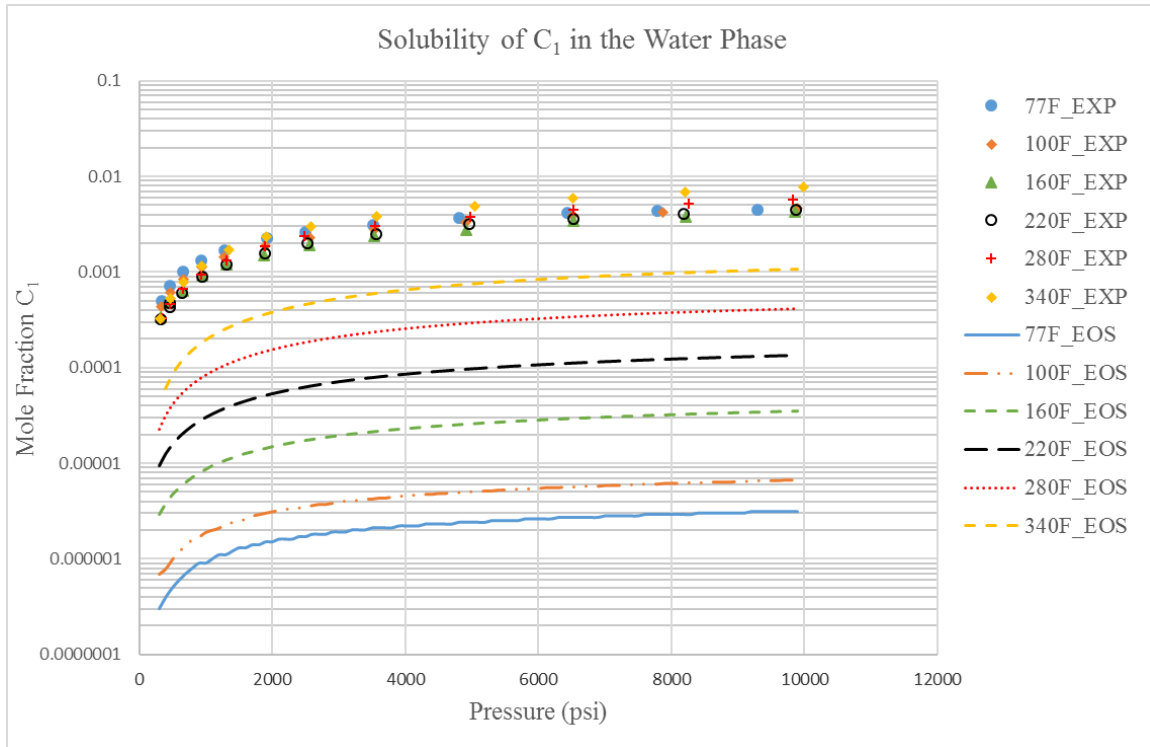


Figure 3-8 Predicted C_1 Solubility in the Water Phase for the Water- C_1 Binary System from a Single EOS Model

3.1.3 Water- C_2

Table 3-3 Component Properties for Water- C_2 Binary System

Component	P_c (psia)	T_c (°F)	v_c (ft ³ /lb-mol)	MW	ω
C_2	708.345	90.05	2.371	30.07	0.098
H_2O	3197.838	705.47	0.897	18.015	0.344

Phase equilibria for a water- C_2 mixture are computed at temperatures from 100 °F to 460 °F and pressure to 10,000 psia with component properties provided in Table 3-3. Experimental data for water vaporization are obtained from Reamer et al. (1943) and data for C_1 composition in the water phase are from Culbertson and McKetta (1950). As shown in Figures 3-9 and 3-10 for the comparisons of calculated and experimental values, very good agreements for both vaporized water in gas and dissolved C_2 in water compositions are attained. The calculated results

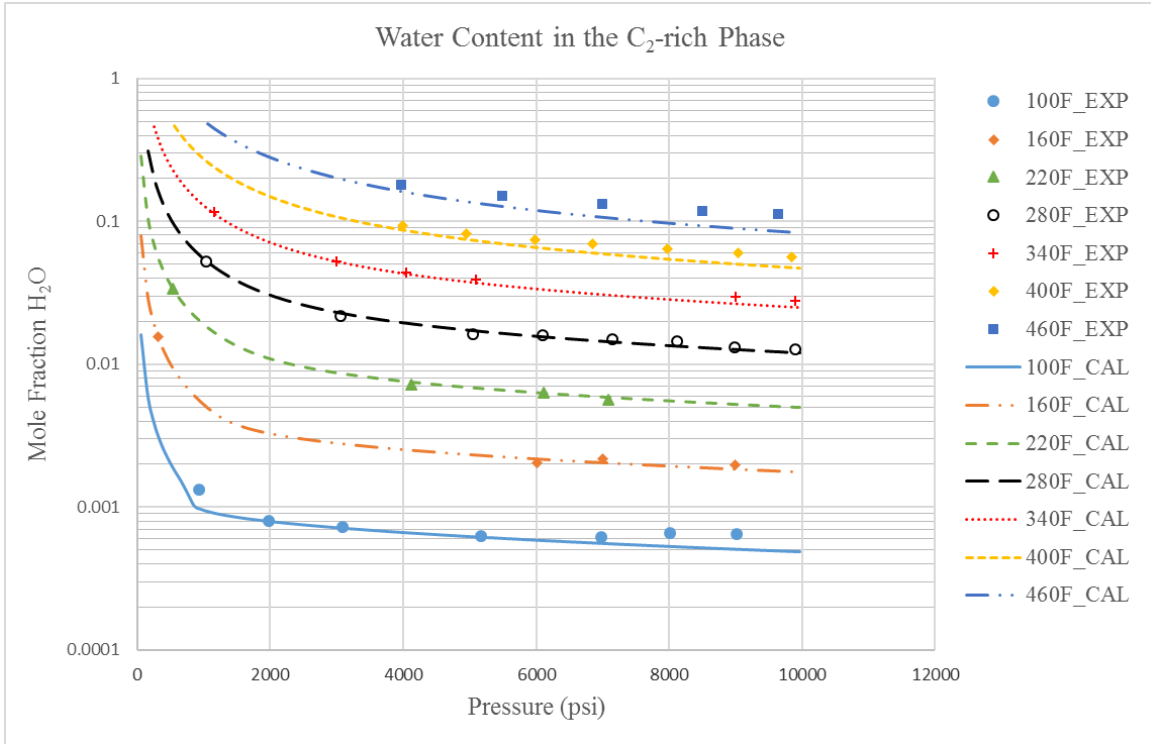


Figure 3-9 Predicted Water Content in the C₂-rich Phase for the Water-C₂ Binary System from this Work

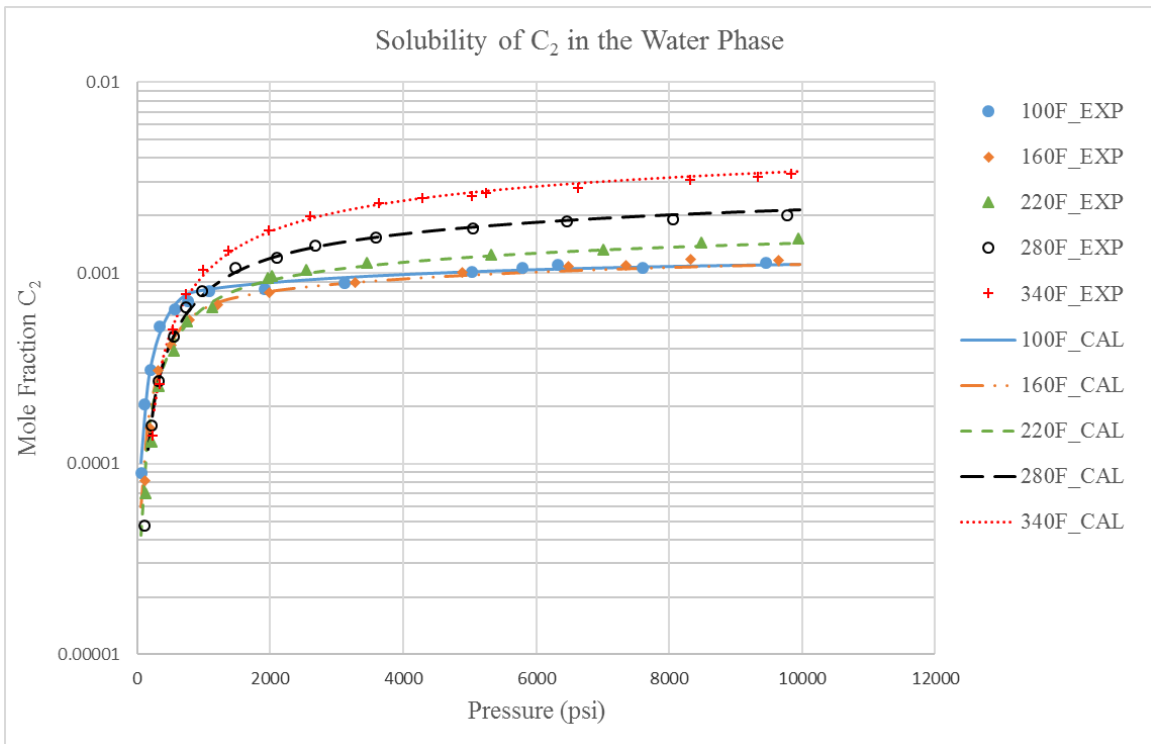


Figure 3-10 Predicted C₂ Solubility in the Water Phase for the Water-C₂ Binary System from this Work

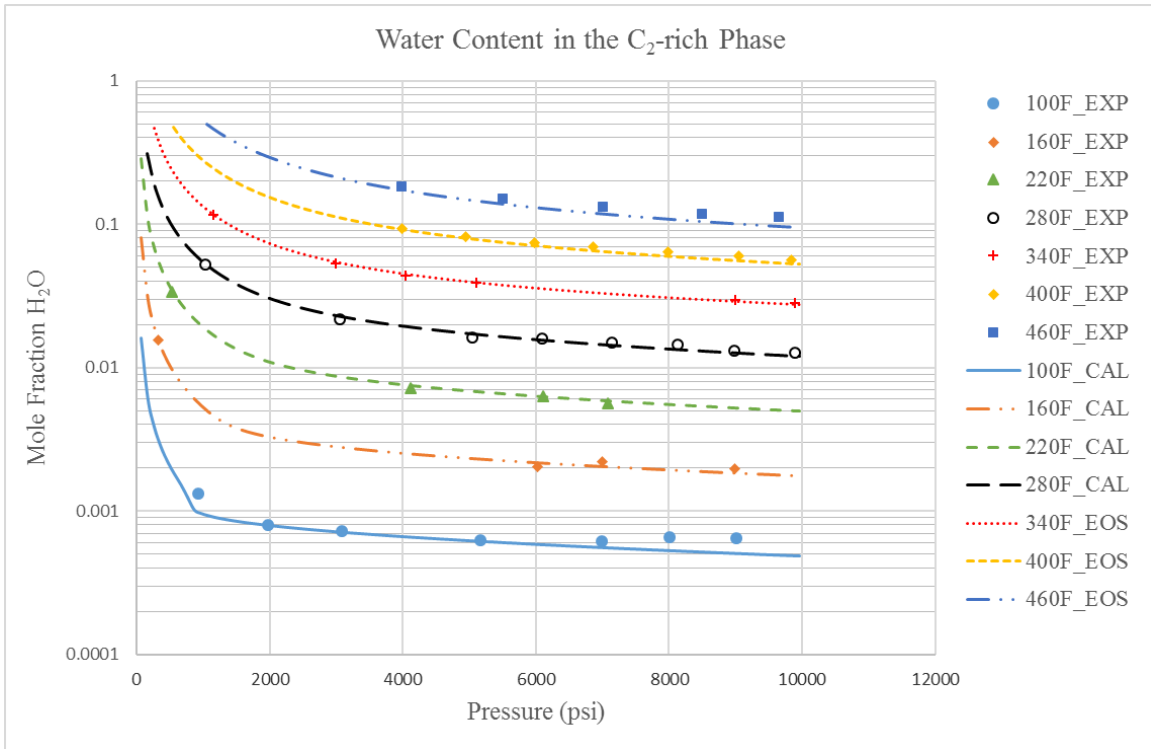


Figure 3-11 Predicted Water Content in the C₂-rich Phase for the Water-C₂ Binary System from a Single EOS Model

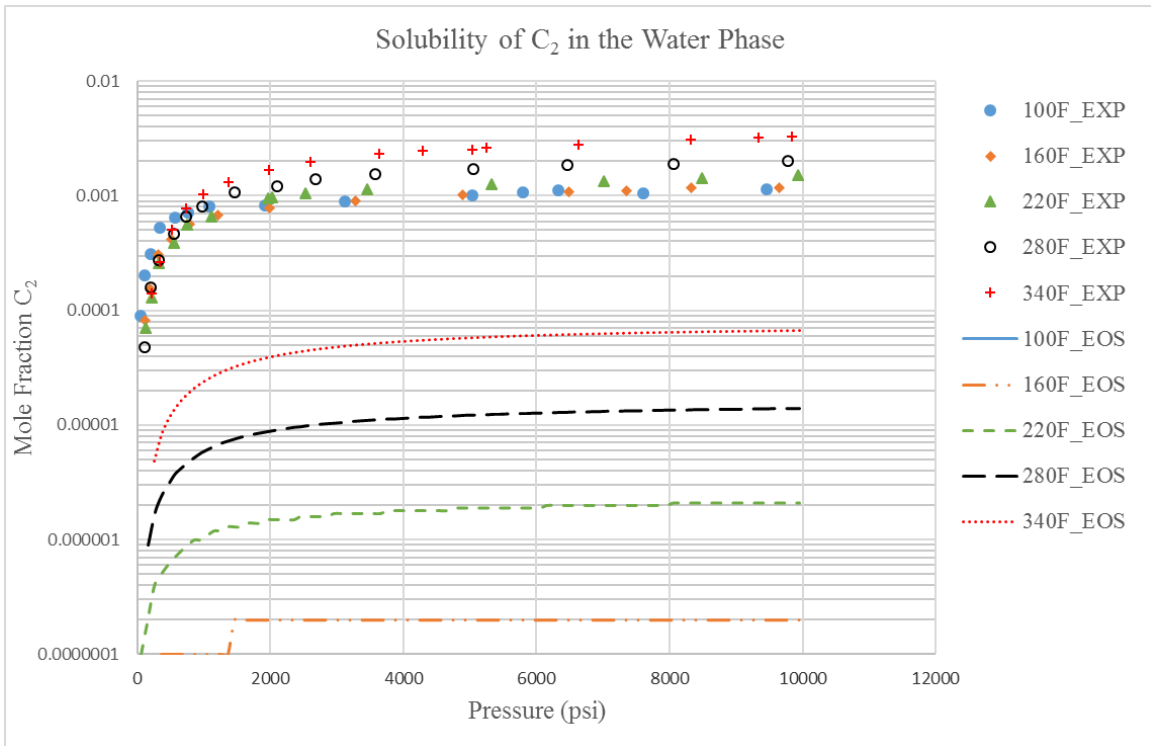


Figure 3-12 Predicted C₂ Solubility in the Water Phase for the Water-C₂ Binary System from a Single EOS Model

from a single EOS model are compared with experimental data in Figures 3-11 and 3-12. The match for the water content in the C₂-rich phase is quite good; however, the prediction of C₂-in-water composition is extremely small and not physical.

3.1.4 Water-C₃

Table 3-4 Component Properties for the Water-C₃ Binary System

Component	P_c (psia)	T_c (°F)	v_c (ft ³ /lb-mol)	MW	ω
C ₃	615.758	205.97	3.252	44.097	0.152
H ₂ O	3197.838	705.47	0.897	18.015	0.344

Phase equilibrium calculations for a water-C₃ binary system are performed at temperature from 54 °F to 212 °F and pressure to 3000 psia. The component properties input can be found in Table 3-4. Calculated phase compositions at equilibrium for both C₃-rich and water phases are compared to laboratory measured data from Kobayashi and Katz (1953) in Figures 3-13 and 3-14. Our algorithm gives an excellent match with experimental data for both water-in-C₃ and C₃-in-water contents. The water content in the C₃-rich phase predicted by a single EOS model also matches well with the experimental values as shown in Figure 3-15. However, similar to other binary systems investigated, the calculated C₃-in-water composition is smaller in orders of magnitudes.

3.2 Water-containing Multicomponent Systems

Laboratory observation has demonstrated multiphase behavior including oil, gas and a second solvent-rich liquid phase during low-temperature CO₂ or rich gas flooding (Huang and Tracht, 1974; Shelton and Yarborough, 1977; Metcalfe and Yarborough, 1979; Orr and Jensen, 1984; Turek *et al.*, 1988; Khan *et al.*, 1992). Considering that water exists universally in a reservoir, either initially in place or as an injected fluid, up to four phases can potentially coexist at

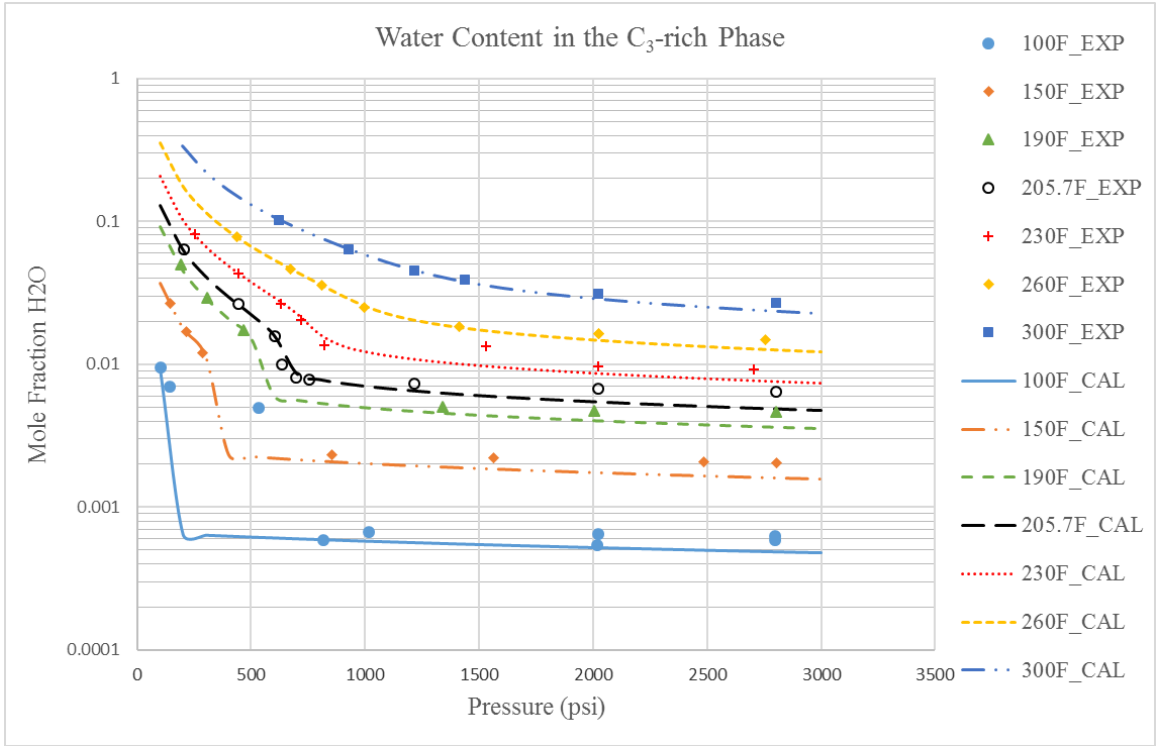


Figure 3-13 Predicted Water Content in the C₃-rich Phase for the Water-C₃ Binary System from this Work

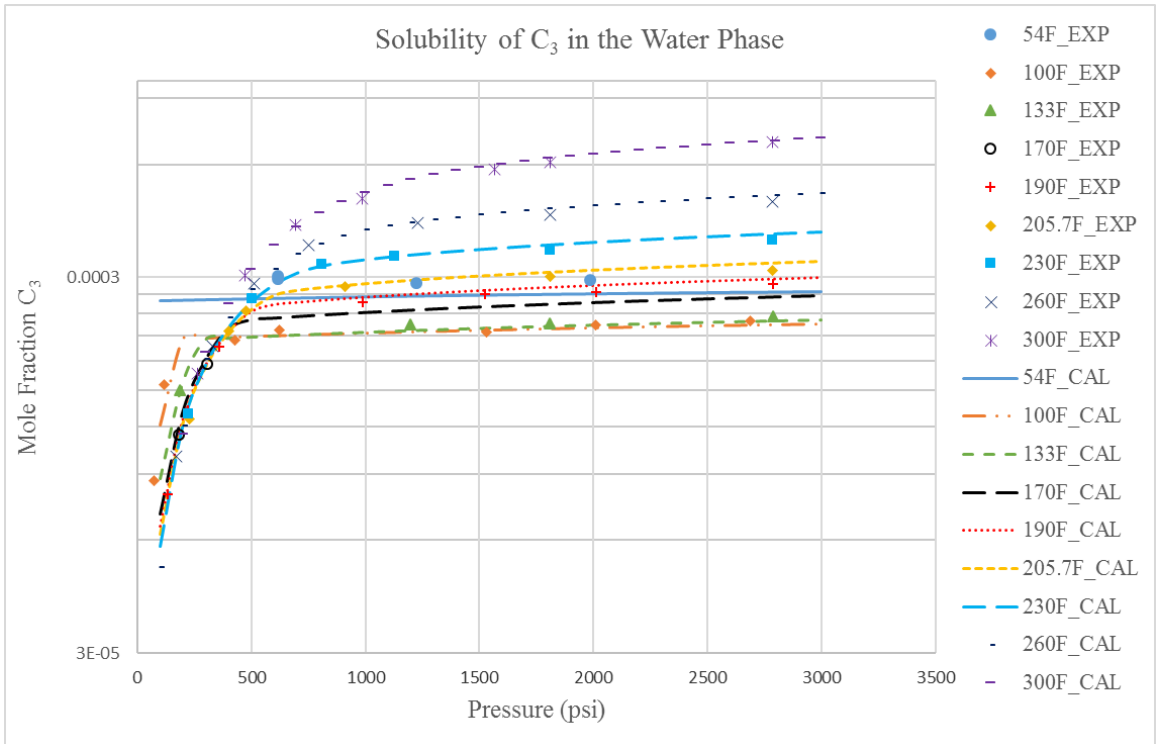


Figure 3-14 Predicted C₃ Solubility in the Water Phase for the Water-C₃ Binary System from this Work

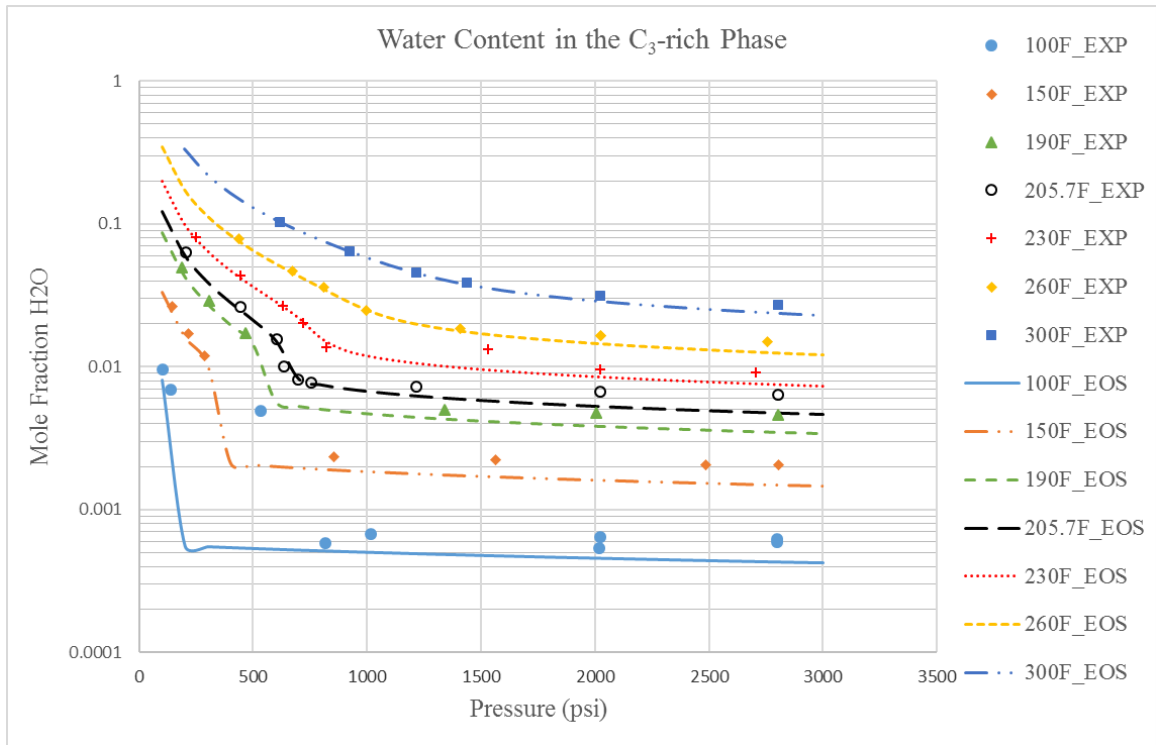


Figure 3-15 Predicted Water Content in the C₃-rich Phase for the Water-C₃ Binary System from a Single EOS Model

equilibrium. In this section, equilibria for multiple hydrocarbon phases are calculated using the algorithm developed in this thesis with water vaporization and solvent/hydrocarbon solubility considered.

3.2.1 16-Component Water-CO₂-Oil Mixture

A three-phase flash calculation case taken from CMG-Winprop templates is investigated. Winprop is an equation of state multiphase equilibrium and properties determination program developed by Computer Modelling Group (CMG) Ltd. (Winprop, 2014) and its results are always considered as industrial references. The original mixture contains 14 hydrocarbons and CO₂. 10% water is added to the system and the compositions of other components are normalized. This case was studied by Wei (2015) and the PR EOS was used to model all the phases including water. An excellent match with Winprop's results was achieved by a single EOS model. However, the predicted solubility of light hydrocarbons and CO₂ in water is very small. Here, we recalculate

phase equilibria of this system using the algorithm developed in this thesis. The PR EOS is applied to compute the component fugacities in the hydrocarbon phases and Henry's law constants are used to calculate the fugacities of solutes in water. Input data for component properties, compositions and binary interaction coefficients can be found in Tables 3-5 and 3-6. The phase equilibria are computed at 94°F and pressure between 1,100 psia and 1,200 psia. The calculated phase mole fractions are shown in Figure 3-16 and compared with the results obtained from a single EOS model as Wei (2015) developed. Both models give the same changes in phase behavior as pressure increases. A CO₂-rich liquid phase is formed at 1,160 psia and four phases are at equilibrium. When the pressure keeps increasing, the amount of the gas phase decreases and it vanishes at 1,185 psia. The mole fraction of the water phase does not change and the oil phase first grows and then begins to shrink slowly after the CO₂-rich liquid appears. The single EOS predicts slightly higher mole fractions of the gas and CO₂-rich liquid, and a lower amount of the water phase than our algorithm does. Since the calculated values of gas solubility in water from a single EOS are always low, more light components, CO₂ and N₂ remain in the hydrocarbon phases compared to the results from Henry's law. Figure 3-17 shows the predicted CO₂, N₂ and hydrocarbon compositions in the water phase. The composition of dissolved gas in water calculated from a single EOS model is smaller by 2 orders of magnitude than our algorithm does. In contrast, the differences in the calculated water composition in the oil, gas and CO₂-rich liquid phases are smaller. As shown in Figure 3-18, our algorithm predicts slightly larger amounts of water in all the other phases. The difference in the oil phase is around 25% and less than 10% for the gas and CO₂-rich liquid phases. However, the absolute values of the difference are negligible.

Table 3-5 Component properties and overall composition for the sixteen-component water-CO₂-hydrocarbon mixture

Comp	P_c (psia)	T_c (°F)	v_c (ft ³ /lbmol)	MW	ω	z_i Water-in	z_i Water-Free
CO ₂	1069.87	87.89	1.5058	44.01	0.225	0.71055	0.7895
N ₂	492.31	-232.51	1.4337	28.013	0.04	0.0009	0.001
C ₁	667.2	-116.59	1.5859	16.043	0.008	0.030915	0.03435
C ₂	708.35	-90.05	2.3708	30.07	0.098	0.007641	0.00849
C ₃	615.76	205.97	3.2518	44.097	0.152	0.005634	0.00626
iC ₄	529.05	274.91	4.2129	58.124	0.176	0.000684	0.00076
nC ₄	551.1	305.69	4.0848	58.124	0.193	0.006237	0.00693
iC ₅	490.85	369.05	4.9017	72.151	0.227	0.002997	0.00333
nC ₅	489.37	385.61	4.8697	72.151	0.251	0.004077	0.00453
nC ₆	430.59	453.65	5.9269	86.178	0.296	0.0063	0.007
C ₇ -C ₁₁	393.85	598.73	6.1031	121.77	0.36958	0.049599	0.05511
C ₁₂ -C ₁₆	289.31	798.584	10.0277	191.8	0.54918	0.029799	0.03311
C ₁₇ -C ₂₂	217.76	927.14	14.1606	267.75	0.6958	0.020448	0.02272
C ₂₃ -C ₂₉	168.77	1046.41	18.7419	357.38	0.95945	0.01233	0.0137
C ₃₀₊	111.94	1260.82	22.4839	549.6	1.2843	0.011889	0.01321
H ₂ O	3197.84	705.47	0.8971	18.015	0.344	0.1	0.0

Table 3-6 Binary interaction parameters for the sixteen-component water-CO₂-hydrocarbon mixture

	CO ₂	N ₂	C ₁	C ₂	C ₃	iC ₄	nC ₄	iC ₅	nC ₅	nC ₆	C ₇ - C ₁₁	C ₁₂ - C ₁₆	C ₁₇ - C ₂₂	C ₂₃ - C ₂₉	C ₃₀₊	H ₂ O
CO ₂	0.0	-0.02	0.1	0.13	0.135	0.13	0.13	0.125	0.125	0.125	0.12	0.12	0.12	0.12	0.12	0.2
N ₂	-0.02	0.0	0.1	0.042	0.091	0.095	0.095	0.095	0.095	0.1	0.1	0.1	0.1	0.1	0.1	0.275
C ₁	0.1	0.1	0.0	0.002	0.007	0.013	0.012	0.017	0.017	0.024	0.025	0.045	0.063	0.079	0.09	0.491
C ₂	0.13	0.042	0.002	0.0	0.001	0.005	0.004	0.007	0.007	0.012	0.012	0.028	0.043	0.057	0.066	0.491
C ₃	0.135	0.091	0.007	0.001	0.0	0.001	0.001	0.002	0.002	0.005	0.005	0.017	0.029	0.041	0.05	0.547
iC ₄	0.13	0.095	0.013	0.005	0.001	0.0	0.0	0.0	0.0	0.002	0.002	0.01	0.02	0.03	0.038	0.508
nC ₄	0.13	0.095	0.012	0.004	0.001	0.0	0.0	0.0	0.0	0.002	0.002	0.011	0.021	0.031	0.039	0.508
iC ₅	0.125	0.095	0.017	0.007	0.002	0.0	0.0	0.0	0.0	0.001	0.001	0.007	0.015	0.024	0.031	0.5
nC ₅	0.125	0.095	0.017	0.007	0.002	0.0	0.0	0.0	0.0	0.001	0.001	0.007	0.016	0.025	0.032	0.5
nC ₆	0.125	0.1	0.024	0.012	0.005	0.002	0.002	0.001	0.001	0.0	0.0	0.004	0.01	0.018	0.024	0.45
C ₇ -C ₁₁	0.12	0.1	0.025	0.012	0.005	0.002	0.002	0.001	0.001	0.0	0.0	0.003	0.01	0.017	0.023	0.0
C ₁₂ -C ₁₆	0.12	0.1	0.045	0.028	0.017	0.01	0.011	0.007	0.007	0.004	0.003	0.0	0.002	0.005	0.009	0.0
C ₁₇ -C ₂₂	0.12	0.1	0.063	0.043	0.029	0.02	0.021	0.015	0.016	0.01	0.01	0.002	0.0	0.001	0.003	0.0
C ₂₃ -C ₂₉	0.12	0.1	0.079	0.057	0.041	0.03	0.031	0.024	0.025	0.018	0.017	0.005	0.001	0.0	0.0	0.0
C ₃₀₊	0.12	0.1	0.09	0.066	0.05	0.038	0.039	0.031	0.032	0.024	0.023	0.009	0.003	0.0	0.0	0.0
H ₂ O	0.2	0.275	0.491	0.491	0.547	0.508	0.508	0.5	0.5	0.45	0.0	0.0	0.0	0.0	0.0	0.0

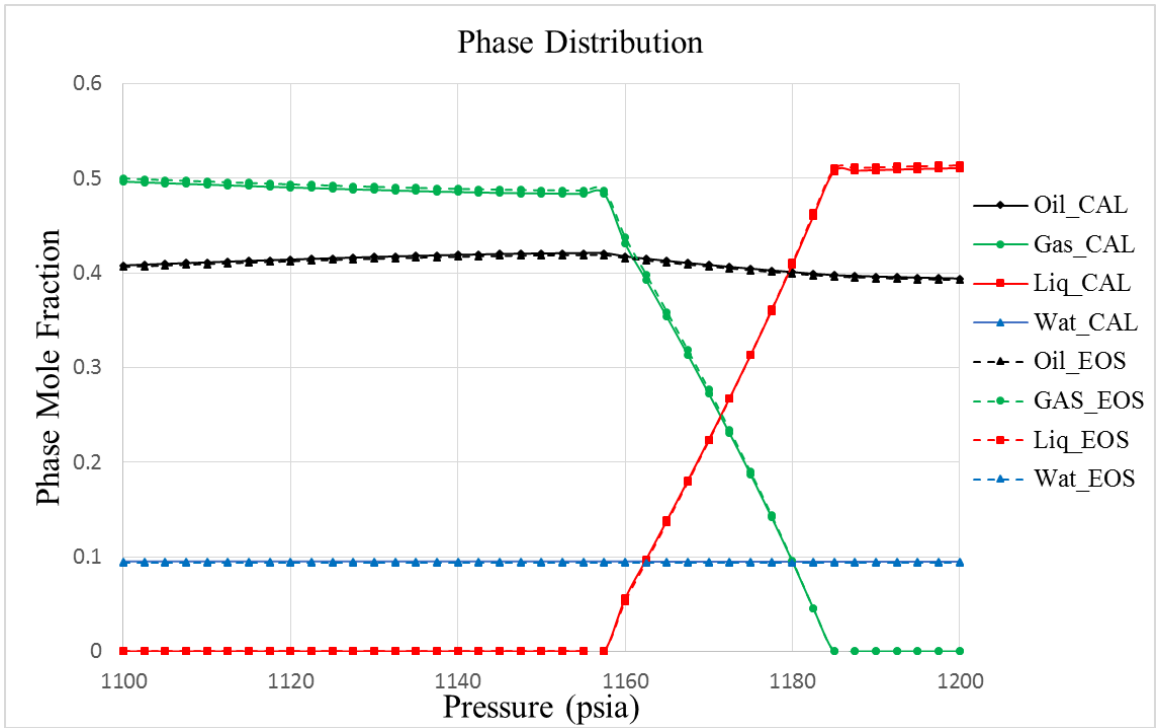


Figure 3-16 Predicted Phase Distribution for the 16-Component Water-CO₂-Oil Mixture

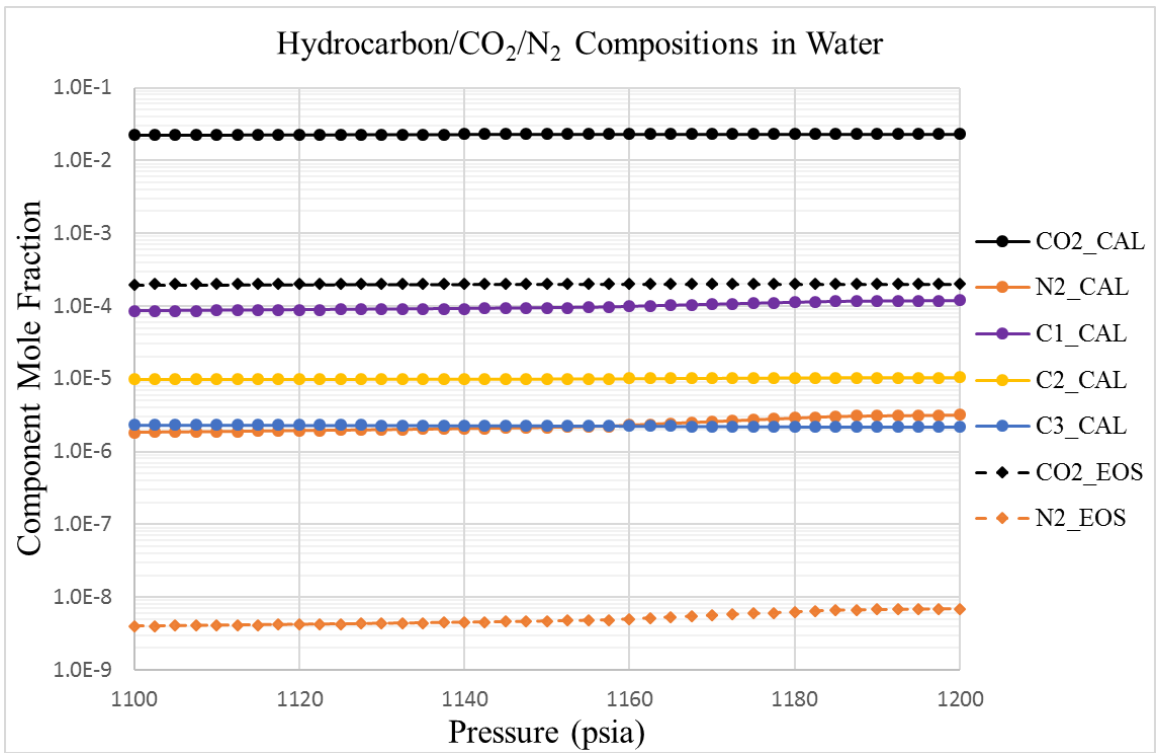


Figure 3-17 Predicted CO₂, N₂ and Hydrocarbon Compositions in the Water Phase for the 16-Component Water-CO₂-Oil Mixture

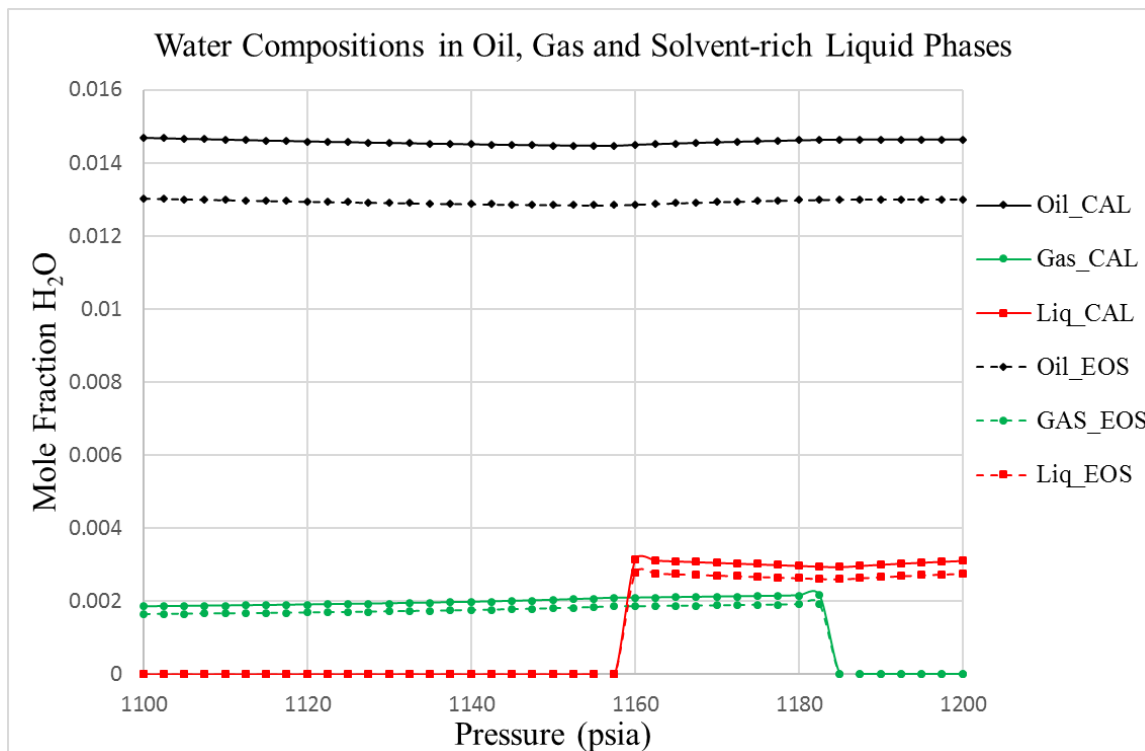


Figure 3-18 Predicted Water Compositions in the Oil, Gas and Solvent-rich Liquid Phases for the 16-component Water-CO₂- Oil Mixture

Our algorithm is compared with Winprop in the prediction of complex phase equilibria. For the Winprop setting, Li-Nghiem's method is specified for the aqueous phase in the component selection/properties and an oil-gas-water (OGW) flash is selected from the dropdown box of flash type in the OGW/EOS multiphase flash to ensure that the same thermodynamic models are used in both programs. Tables 3-7, 3-8 and 3-9 present the calculated phase mole fractions and compositions at the pressures of 1100 psia, 1170 psia and 1200 psia, respectively. They show that the agreements on the predicted phase equilibria calculated from our algorithm and Winprop are excellent at 1,100 psia and 1,200 psia which correspond to the liquid-vapor and liquid-liquid equilibria. However, at 1,170 psia, Winprop exhibits the limitation in handling both multi-phases and water. Only three-phase oil-gas-water equilibrium is obtained when four-phase equilibrium is

expected. The incorrect number of phases makes the prediction of phase amounts and phase compositions by Winprop invalid since the minimization of Gibbs free energy is not satisfied.

Table 3-7 Predicted Phase Mole Fractions and Compositions at 94 °F and 1,100 psia for the for the 16-Component Water-CO₂- Oil Mixture

Phase	Oil Mole %		Gas Mole %		CO ₂ -rich Liquid Mole %		Water Mole %	
	This Work	WinProp	This Work	WinProp	This Work	WinProp	This Work	WinProp
Phase	40.8085	40.7978	49.6661	49.6698	0.0	0.0	9.5254	9.5324
CO ₂	60.7731	60.77341	92.69617	92.69735	0.0	0.0	2.26597	2.28902
N ₂	0.03168	0.03168	0.15515	0.15514	0.0	0.0	0.00018	0.00017
C ₁	1.84189	1.84201	4.70953	4.70947	0.0	0.0	0.00852	0.00856
C ₂	0.83918	0.83930	0.84877	0.84878	0.0	0.0	0.00099	0.00100
C ₃	0.84498	0.84515	0.44005	0.44005	0.0	0.0	0.00023	0.00024
iC ₄	0.11925	0.11928	0.03973	0.03973	0.0	0.0	0.00001	0.00001
nC ₄	1.14716	1.14742	0.31320	0.31320	0.0	0.0	0.00010	0.00010
iC ₅	0.60749	0.60764	0.10428	0.10428	0.0	0.0	0.00001	0.00001
nC ₅	0.84645	0.84666	0.12539	0.12539	0.0	0.0	0.00001	0.00001
nC ₆	1.40301	1.40337	0.11568	0.11567	0.0	0.0	0.0	0.0
C ₇ -C ₁₁	11.8441	11.84716	0.25465	0.25471	0.0	0.0	0.0	0.0
C ₁₂ -C ₁₆	7.28840	7.29030	0.01130	0.01131	0.0	0.0	0.0	0.0
C ₁₇ -C ₂₂	5.00954	5.01085	0.00097	0.00097	0.0	0.0	0.0	0.0
C ₂₃ -C ₂₉	3.02140	3.02219	0.00002	0.00002	0.0	0.0	0.0	0.0
C ₃₀₊	2.91337	2.91413	0.0	0.0	0.0	0.0	0.0	0.0
H ₂ O	1.46889	1.45943	0.18511	0.18393	0.0	0.0	97.72396	97.70087

Table 3-8 Predicted Phase Mole Fractions and Compositions at 94 °F and 1,170 psia for the for the 16-Component Water-CO₂- Oil Mixture

Phase	Oil Mole %		Gas Mole %		CO ₂ -rich Liquid Mole %		Water Mole %	
	This Work	WinProp	This Work	WinProp	This Work	WinProp	This Work	WinProp
Phase	40.8629	41.6144	27.2729	48.8764	22.3666	0.0	9.4975	9.5092
CO ₂	61.66072	61.87410	92.08678	92.24515	91.77182	0.0	2.29137	2.31741
N ₂	0.04488	0.04342	0.17139	0.14713	0.11130	0.0	0.00026	0.00023
C ₁	2.27932	2.23021	4.90735	4.42428	3.66941	0.0	0.01054	0.01035
C ₂	0.86113	0.85714	0.84729	0.83335	0.80942	0.0	0.00102	0.00102
C ₃	0.79721	0.80049	0.45091	0.47110	0.51254	0.0	0.00022	0.00022
iC ₄	0.10870	0.10959	0.04279	0.04664	0.05504	0.0	0.00001	0.00001
nC ₄	1.03828	1.04888	0.34521	0.38302	0.47067	0.0	0.00009	0.00010
iC ₅	0.54437	0.55101	0.12436	0.14403	0.19377	0.0	0.00001	0.00001
nC ₅	0.75889	0.76847	0.15336	0.17985	0.24934	0.0	0.00001	0.00001
nC ₆	1.27040	1.28450	0.15889	0.19532	0.30198	0.0	0.0	0.0
C ₇ -C ₁₁	11.11950	11.17671	0.46081	0.63176	1.29868	0.0	0.0	0.0
C ₁₂ -C ₁₆	7.16099	7.09263	0.03444	0.05800	0.19815	0.0	0.0	0.0
C ₁₇ -C ₂₂	4.97552	4.90284	0.00456	0.00923	0.04656	0.0	0.0	0.0
C ₂₃ -C ₂₉	3.01444	2.96228	0.00020	0.00055	0.00517	0.0	0.0	0.0
C ₃₀₊	2.90929	2.85693	0.00000	0.00001	0.00034	0.0	0.0	0.0
H ₂ O	1.45636	1.44080	0.21166	0.23059	0.30581	0.0	97.69645	97.67062

Table 3-9 Predicted Phase Mole Fractions and Compositions at 94 °F and 1,200 psia for the for the 16-Component Water-CO₂- Oil Mixture

Phase	Oil Mole %		Gas Mole %		2 nd Liquid Mole %		Water Mole %	
	This Work	WinProp	This Work	WinProp	This Work	WinProp	This Work	WinProp
Phase	39.4251	39.4156	0.0	0.0	51.0928	51.0950	9.4821	9.4894
CO ₂	61.33951	61.34029	0.0	0.0	91.31363	91.31583	2.29001	2.31332
N ₂	0.05525	0.05524	0.0	0.0	0.13346	0.13347	0.00032	0.00030
C ₁	2.56847	2.56851	0.0	0.0	4.06661	4.06687	0.01192	0.01198
C ₂	0.87495	0.87506	0.0	0.0	0.82018	0.82022	0.00104	0.00105
C ₃	0.77732	0.77748	0.0	0.0	0.50285	0.50285	0.00022	0.00022
iC ₄	0.10426	0.10429	0.0	0.0	0.05342	0.05342	0.00001	0.00001
nC ₄	0.99079	0.99103	0.0	0.0	0.45617	0.45615	0.00009	0.00009
iC ₅	0.51661	0.51675	0.0	0.0	0.18794	0.18792	0.00001	0.00001
nC ₅	0.72001	0.72020	0.0	0.0	0.24237	0.24235	0.00001	0.00001
nC ₆	1.21260	1.21294	0.0	0.0	0.29737	0.29731	0.0	0.0
C ₇ -C ₁₁	10.84915	10.85195	0.0	0.0	1.33603	1.33583	0.0	0.0
C ₁₂ -C ₁₆	7.27461	7.27647	0.0	0.0	0.21898	0.21889	0.0	0.0
C ₁₇ -C ₂₂	5.11769	5.11896	0.0	0.0	0.05314	0.05310	0.0	0.0
C ₂₃ -C ₂₉	3.11948	3.12024	0.0	0.0	0.00615	0.00614	0.0	0.0
C ₃₀₊	3.01504	3.01577	0.0	0.0	0.00043	0.00043	0.0	0.0
H ₂ O	1.46426	1.45482	0.0	0.0	0.31127	0.30921	97.69637	99.97989

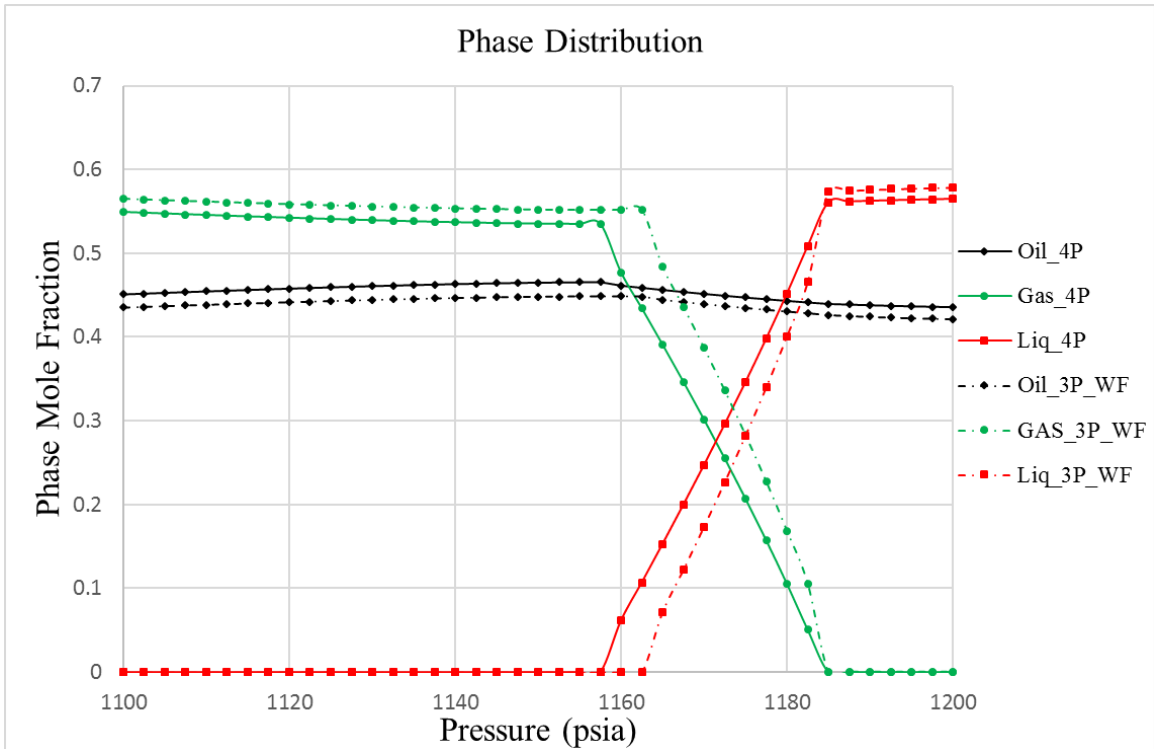


Figure 3-19 Comparisons of 3-Phase Water-free and 4-Phase Water-in Equilibrium Calculations for the 16-component Water-CO₂-Oil Mixture

To investigate the effect of water on the phase behavior of hydrocarbon phases, water-free equilibrium calculations are carried out in the same pressure range. For comparison, the water-free calculation results are plotted in Figure 3-19 with normalized phase mole fractions obtained from 4-phase water-in calculations. The phase mole fractions are normalized by

$$\beta_j = \frac{\beta_j}{1 - \beta_w}, \quad j = o, g, l$$

It is observed that the water-free calculation obtains larger mole fractions of gas and the CO₂-rich liquid phase in the two-phase region since these two phases majorly consist of CO₂ and a certain amount of CO₂ is predicted dissolving in water by water-in calculations. The three-phase region predicted by the water-free equilibrium calculation is narrower than that from the four-phase calculation. The CO₂-rich liquid first appears at 1,165 psia, and the pressures at which the gas

phase disappears are the same for both calculations. In addition to forming the water phase, the existence of the water component in the system also expands the pressure range of the liquid-liquid-vapor equilibrium. Similar observation was presented by Wei (2015). However, the single EOS model does not represent the water phase properly. It is difficult to judge the reliability of his four-phase water-in calculation results.

3.2.2 12-Component Water-CO₂-Wasson Oil Mixture

Multiphase behavior for a recombined oil (dead oil + 312 SCF/BBL gas) from the Wasson field originally described by Orr and Jensen (1984) is investigated. The fluid characterization represented by 10 hydrocarbon components is taken from Nghiem and Li (1986) and it was reported that these components are adequate to predict important features including liquid-vapor, liquid-liquid-vapor and liquid-liquid equilibria shown in an experimental phase diagram. 85% CO₂ is first introduced into the system and the originally characterized hydrocarbon compositions are normalized accordingly. 20% water is then added to the CO₂-crude oil system and another normalization is performed. The component properties, feed compositions and binary interaction coefficients are listed in Table 3-10. Multiphase equilibrium calculations are carried out at 90 °F and pressure from 1,050 psia to 1,150 psia. The PR EOS is used to represent hydrocarbon phases and Henry's law is used for the water phase.

The predicted phase mole fractions are presented in Figure 3-20, together with the results obtained from a single EOS model that uses the PR EOS for both the hydrocarbon and water phases. Both results exhibit the same phase transition that starts from liquid-vapor-water equilibrium, then passes through the liquid-liquid-vapor-water zone and finally switches to liquid-liquid-water equilibrium. The CO₂-rich liquid phase first appears at 1,077.5 psia where the gas phase begins to diminish. The amount of the CO₂-rich liquid phase keeps increasing and the amounts of the oil and gas phases decrease as pressure increases. The gas phase mole fraction

Table 3-10 Component Properties, Feed Compositions and Binary Interaction Coefficient for 12-Component Water-CO₂-Wasson Oil Mixture

Component Properties and Feed Compositions

Comp	P_c (psia)	T_c (°F)	v_c (ft ³ /lb-mol)	MW	ω	z_i Original	z_i CO ₂ -in	z_i Water-in
C ₁	667.1960	-116.59	1.585855	16.043	0.008	0.2151	0.032265	0.025812
C ₂	708.3447	90.05	2.370773	30.07	0.098	0.0746	0.01119	0.008952
C ₃	615.7603	205.97	3.251803	44.097	0.152	0.0611	0.009165	0.007332
C ₄	551.0981	305.69	4.084778	58.124	0.193	0.0242	0.00363	0.002904
C ₅	489.3751	385.61	4.869696	72.151	0.251	0.0343	0.005145	0.004116
C ₆	477.0305	453.83	5.510445	86.178	0.2637	0.0336	0.00504	0.004032
C ₇₋₁₃	384.5930	632.03	7.833163	125.96	0.3912	0.3	0.045	0.036
C ₁₄₋₂₀	248.2146	872.33	13.64796	227.86	0.63	0.1066	0.01599	0.012792
C ₂₁₋₂₈	181.3480	1022.8 1	18.91813	325.56	0.8804	0.0552	0.00828	0.006624
C ₂₉₊	116.9798	1206.9 5	28.22501	484.7	1.2457	0.0953	0.014295	0.011436
CO ₂	1069.865	87.89	1.505761	44.01	0.2250	0.0	0.85	0.68
H ₂ O	3197.84	705.47	0.8971	18.015	0.344	0.0	0.0	0.2

Binary interaction coefficients:

	C ₁	C ₂	C ₃	C ₄	C ₅	C ₆	C ₇₋₁₃	C ₁₄₋₂₀	C ₂₁₋₂₈	C ₂₉₊	CO ₂	H ₂ O
C ₁	0.0	0.003	0.009	0.015	0.021	0.025	0.041	0.073	0.095	0.125	0.103	0.4907
C ₂	0.003	0.0	0.002	0.005	0.009	0.012	0.023	0.049	0.068	0.095	0.13	0.4911
C ₃	0.009	0.002	0.0	0.001	0.003	0.005	0.013	0.033	0.05	0.073	0.135	0.5469
C ₄	0.015	0.005	0.001	0.0	0.001	0.001	0.007	0.024	0.038	0.059	0.13	0.508
C ₅	0.021	0.009	0.003	0.001	0.0	0.0	0.004	0.017	0.03	0.049	0.125	0.5
C ₆	0.025	0.012	0.005	0.001	0.0	0.0	0.002	0.014	0.025	0.043	0.125	0.45
C ₇₋₁₃	0.041	0.023	0.013	0.07	0.004	0.002	0.0	0.005	0.013	0.027	0.13	0.45
C ₁₄₋₂₀	0.073	0.049	0.033	0.024	0.017	0.014	0.005	0.0	0.002	0.009	0.13	0.45
C ₂₁₋₂₈	0.095	0.068	0.05	0.038	0.03	0.025	0.013	0.002	0.0	0.003	0.13	0.45
C ₂₉₊	0.125	0.095	0.073	0.059	0.049	0.043	0.027	0.009	0.003	0.0	0.13	0.45
CO ₂	0.103	0.13	0.135	0.13	0.125	0.125	0.13	0.13	0.13	0.13	0.0	0.2
H ₂ O	0.4907	0.4911	0.5469	0.508	0.5	0.45	0.45	0.45	0.45	0.45	0.2	0.0

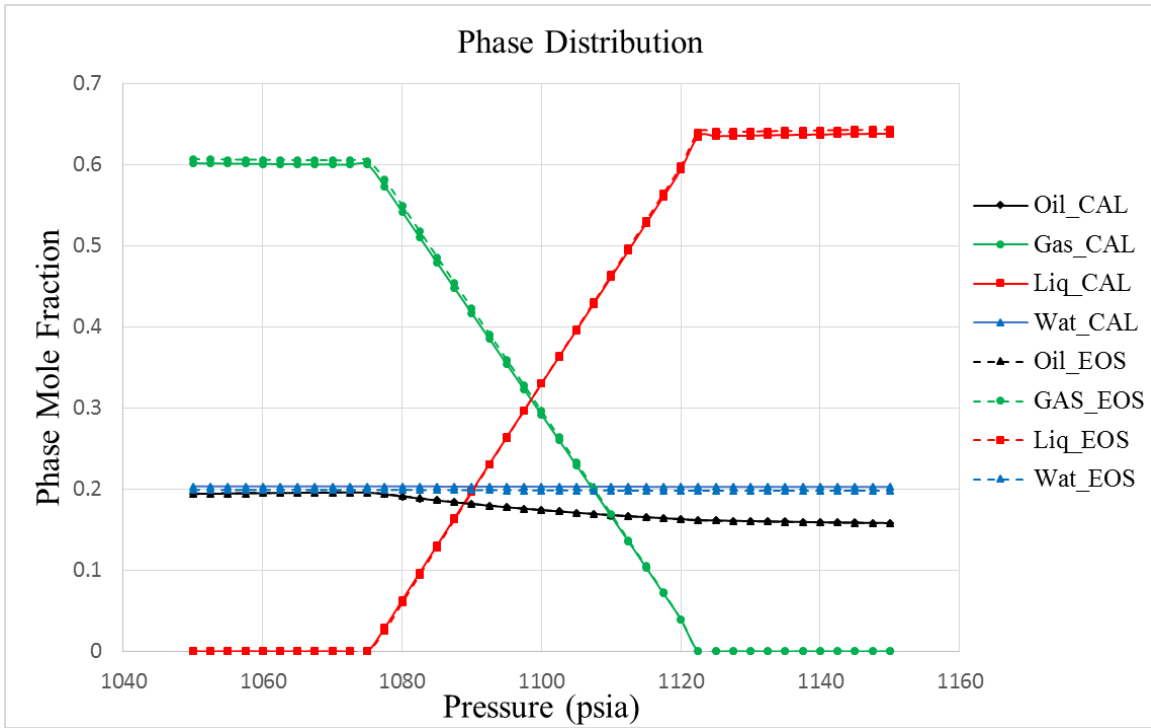


Figure 3-20 Predicted Phase Distribution for the 12-Component Water-CO₂-Wasson Oil Mixture

shrinks more substantially than the oil phase does while the water phase is almost identical over the entire pressure range. The gas phase finally disappears at 1,122.5 psia and the oil, CO₂-rich liquid and water remain at equilibrium. Mole fractions of the gas and CO₂-rich liquid phases calculated from a single EOS model are slightly higher than the prediction made by this work while the amount of the predicted water phase is less because the dissolved hydrocarbons and CO₂ calculated from the EOS are much smaller than those obtained from Henry's law. As shown in Figure 3-20, the calculated CO₂ content in water from a single EOS is smaller by 2 orders of magnitudes and C₁ composition in water is smaller by 3 orders of magnitudes compared to the values estimated by the algorithm developed in this work while the predicted compositions for C₂, C₃, C₄ and C₅ using a single EOS model are all less than 1.0E-08. The predicted water compositions in the oil, gas and CO₂-rich liquid phases are depicted in Figure 3-21. The water vaporization

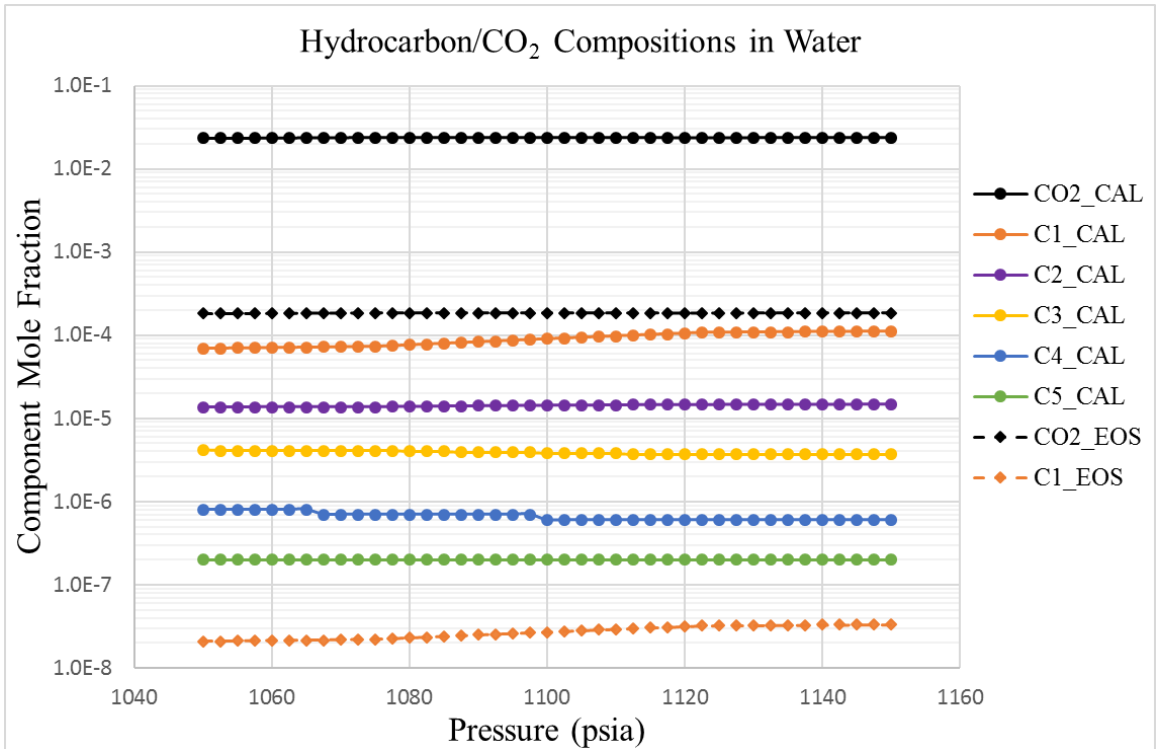


Figure 3-21 Predicted Hydrocarbon and CO₂ Compositions in the Water Phase for the 12-Component Water-CO₂-Wasson Oil Mixture

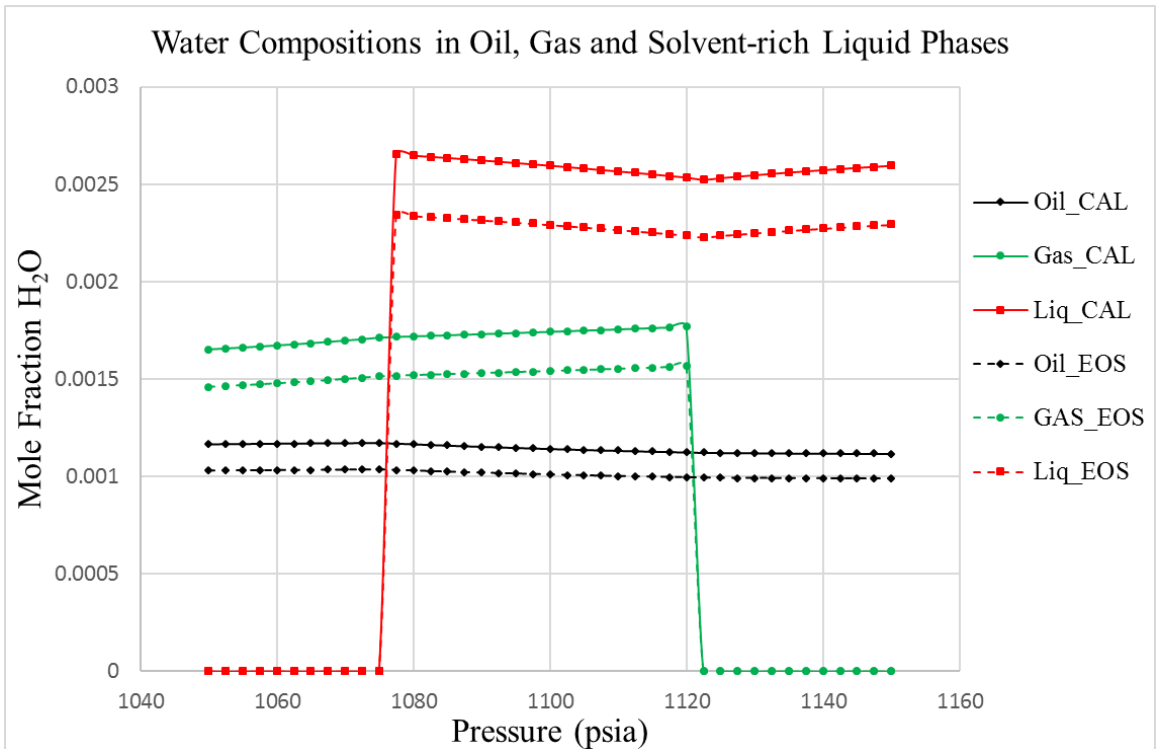


Figure 3-22 Predicted Water Compositions in the Oil, Gas and CO₂-rich Liquid Phases for the 12-Component Water-CO₂-Wasson Oil Mixture

calculated from this work is slightly larger than that predicted by a single EOS model by less than 15%.

Our results are compared to the calculation results from Winprop in Tables 3-11, 3-12 and 3-13 for the phase mole fractions and compositions predicted at 1,050 psia, 1,100 psia and 1150 psia, respectively. They show that our results match very well with Winprop on the predicted phase equilibria calculated at 1,050 psia and 1,150 psia which correspond to liquid-vapor and liquid-liquid equilibria. However, only three-phase oil-gas-water equilibrium is obtained by Winprop at 1,100 psia but the phase diagram depicts three hydrocarbon equilibrium phases at this point (Nghiem and Li, 1986).

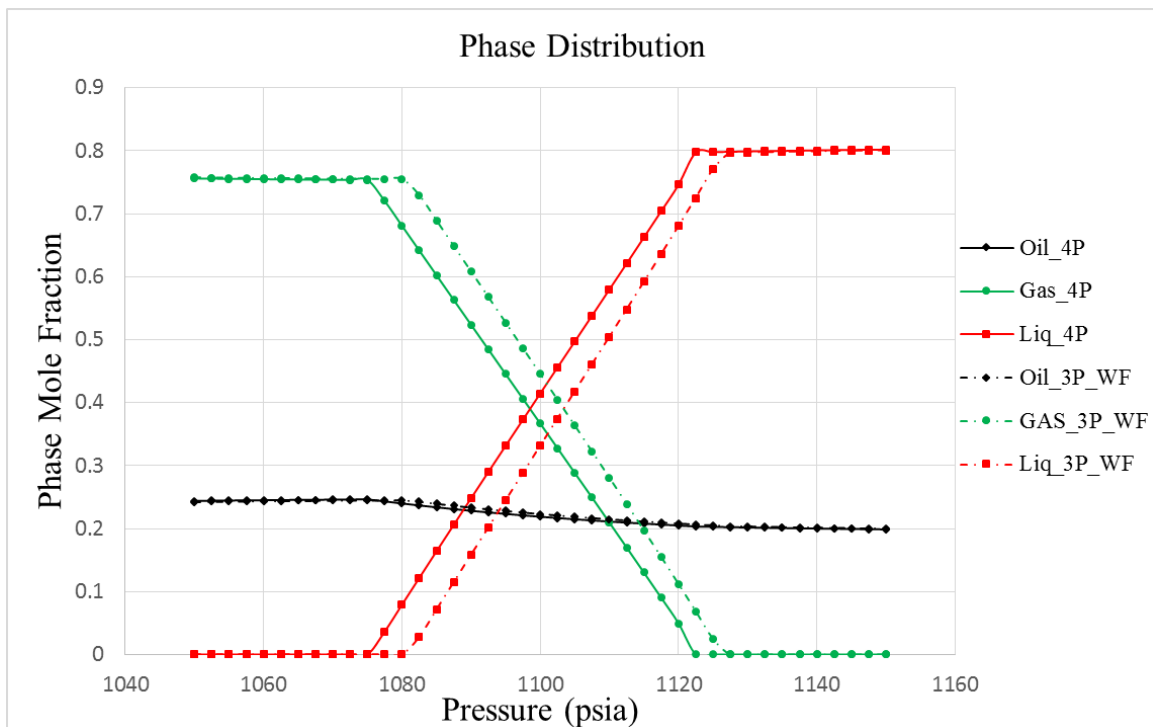


Figure 3-23 Comparisons of 3-Phase Water-free and 4-Phase Water-in Equilibrium Calculations for the 16-Component Water-CO₂-Wasson Oil Mixture

Three-phase water-free calculations are also performed to investigate the effect of water existence on phase behavior. As shown in Figure 3-23, the phase separation predicted by the three-phase water-free calculation enters the multiple-hydrocarbon liquid-liquid-vapor region at 1,082.5

psia which is 5 psia higher than that obtained from four-phase water-in calculations and the oil phase mole fraction from the 3-phase calculation is also slightly higher. It is indicated that the interaction between water and hydrocarbon/CO₂ components and dissolved hydrocarbon/CO₂ in the water phase can shift the multiple phase boundary to a lower pressure.

Table 3-11 Predicted Phase Mole Fractions and Compositions at 90 °F and 1,050 psia for the for the Water-CO₂-Wasson Oil Mixture

Phase	Oil Mole %		Gas Mole %		CO ₂ -rich Liquid, Mole %		Water Mole %	
	This Work	WinProp	This Work	WinProp	This Work	WinProp	This Work	WinProp
Phase	19.4295	19.4163	60.2133	60.2192	0.0	0.0	20.3645	20.3572
C ₁	1.39977	1.3998	3.83274	3.83265	0.0	0.0	0.00693	0.00697
C ₂	1.06939	1.06917	1.14119	1.14137	0.0	0.0	0.00136	0.00137
C ₃	1.42244	1.42188	0.75854	0.75896	0.0	0.0	0.00042	0.00042
C ₄	0.81062	0.81040	0.22069	0.22093	0.0	0.0	0.00008	0.00004
C ₅	1.46716	1.46677	0.21014	0.21058	0.0	0.0	0.00002	0.0
C ₆	1.64637	1.64736	0.13837	0.1384	0.0	0.0	0.0	0.0
C ₇₋₁₃	17.82977	17.84176	0.22547	0.22549	0.0	0.0	0.0	0.0
C ₁₄₋₂₀	6.57701	6.58149	0.00219	0.00219	0.0	0.0	0.0	0.0
C ₁₉₋₂₈	3.40914	3.41146	0.00003	0.00003	0.0	0.0	0.0	0.0
C ₂₉	5.88589	5.88989	0.0	0.0	0.0	0.0	0.0	0.0
CO ₂	58.36588	58.34426	93.30545	93.30529	0.0	0.0	2.34548	2.37676
H ₂ O	0.11656	0.11575	0.16519	0.16411	0.0	0.0	97.64571	97.61444

Table 3-12 Predicted Phase Mole Fractions and Compositions at 90 °F and 1,100 psia for the for the Water-CO₂-Wasson Oil Mixture

	Oil Mole %		Gas Mole %		CO ₂ -rich Liquid Mole %		Water Mole %	
	This Work	WinProp	This Work	WinProp	This Work	WinProp	This Work	WinProp
Phase	17.435	19.3794	29.2215	60.2628	33.0177	0.0	20.3258	20.3578
C ₁	1.79767	1.62139	4.51264	3.7591	2.86902	0.0	0.009	0.00808
C ₂	1.10435	1.08973	1.17086	1.13458	1.09100	0.0	0.00143	0.0014
C ₃	1.29521	1.34936	0.72898	0.78261	0.89129	0.0	0.00038	0.0004
C ₄	0.67857	0.73786	0.20770	0.24459	0.33735	0.0	0.00006	0.00004
C ₅	1.19116	1.32155	0.20420	0.25802	0.43688	0.0	0.00002	0.0
C ₆	1.35549	1.50137	0.14268	0.18626	0.37912	0.0	0.0	0.0
C ₇₋₁₃	16.84523	17.23125	0.31341	0.43258	1.73073	0.0	0.0	0.0
C ₁₄₋₂₀	7.11798	6.57562	0.00487	0.0081	0.11132	0.0	0.0	0.0
C ₁₉₋₂₈	3.78025	3.41733	0.00011	0.00023	0.00994	0.0	0.0	0.0
C ₂₉	6.55672	5.90109	0.0	0.00001	0.00131	0.0	0.0	0.0
CO ₂	58.16315	59.13721	92.54035	93.00947	91.88246	0.0	2.3619	2.40413
H ₂ O	0.11421	0.11625	0.17422	0.18444	0.25958	0.0	97.62716	97.58595

Table 3-13 Predicted Phase Mole Fractions and Compositions at 90 °F and 1,150 psia for the for the Water-CO₂-Wasson Oil Mixture

	Oil Mole %		Gas Mole %		2 nd Liquid Mole %		Water Mole %	
	This Work	WinProp	This Work	WinProp	This Work	WinProp	This Work	WinProp
Phase	15.8317	15.8216	0.0	0.0	63.8693	63.8716	20.2990	20.3068
C ₁	2.19385	2.19386	0.0	0.0	3.49405	3.49425	0.0111	0.01115
C ₂	1.12999	1.12986	0.0	0.0	1.12104	1.12121	0.00148	0.00149
C ₃	1.22026	1.21925	0.0	0.0	0.84538	0.84579	0.00037	0.00037
C ₄	0.60632	0.60585	0.0	0.0	0.30437	0.30458	0.00006	0.00003
C ₅	1.04095	1.03945	0.0	0.0	0.38641	0.38694	0.00002	0.0
C ₆	1.18781	1.18859	0.0	0.0	0.33686	0.33684	0.0	0.0
C ₇₋₁₃	16.00364	16.01549	0.0	0.0	1.66960	1.66912	0.0	0.0
C ₁₄₋₂₀	7.59787	7.60366	0.0	0.0	0.11951	0.11927	0.0	0.0
C ₁₉₋₂₈	4.14057	4.14349	0.0	0.0	0.01077	0.0107	0.0	0.0
C ₂₉	7.21801	7.22263	0.0	0.0	0.00136	0.00135	0.0	0.0
CO ₂	57.54902	57.52693	0.0	0.0	91.45114	91.45217	2.36366	2.3952
H ₂ O	0.11171	0.11092	0.0	0.0	0.25951	0.25778	97.62333	97.59176

Chapter Four: **Conclusions and Recommendations for Future Research**

4.1 Conclusions

In this thesis, a robust multiphase equilibrium calculation algorithm has been developed to model water-hydrocarbon mutual solubility and complex multiphase behavior of a CO₂/rich gas and crude oil mixture simultaneously. This algorithm sequentially applies phase stability tests and phase split calculations to ensure that the calculated equilibrium system satisfies the conditions of material balance and the second law of thermodynamics simultaneously. The water and hydrocarbon phases are computed differently by proper thermodynamic models: A cubic EOS is used to calculate the component fugacities in the hydrocarbon phases and the water phase is modeled by Henry's law.

The calculation results have been validated by both experimental measurements and commercial software. Excellent matches have been achieved for our calculation results compared to experimental data for various binary systems including water-CO₂, water-C₁, water-C₂ and water-C₃ under reservoir conditions. In the liquid-vapor-water and liquid-liquid-water regions, very good agreements of the results obtained from our algorithm and Winprop are achieved as well. In addition, our algorithm is able to predict the three hydrocarbon phase region which is the limitation of the existing commercial software.

The effect of the existence of water in the phase equilibrium calculation is also investigated. The introduction of the water component in the multiphase equilibrium calculation can shift and/or expand the pressure range for the three-phase liquid-liquid-vapor region due to the complex interaction between water and hydrocarbon/CO₂/N₂. It is observed that the substantial amount of dissolved gas in water can also result in the smaller mole fractions of gas and the solvent-rich liquid phase existing in the system for a rigorous water-in equilibrium calculation.

4.2 Recommendations for Future Research

The algorithm in this thesis can be implemented in a four-phase compositional simulator to study the effect of multiphase behavior phenomena and/or water-hydrocarbon mutual solubility on the production of gas and water-alternating-gas injection processes.

Asphaltene precipitation is an important problem in oil and gas production and up to five equilibrium phases can coexist. The calculations of equilibria including a solid phase can use the same workflow as presented in this thesis. However, suitable thermodynamic models for the solid phase should be selected for calculations.

Experiments of multiphase equilibria including the water, hydrocarbon and solvent-rich phases should be conducted to obtain accurate data that can help validating our calculation results of a system of multiple hydrocarbon phases and water.

References

- Abhvani, A. S. and Beaumont, D. N.: "Development of an Efficient Algorithm for the Calculation of Two-Phase Flash Equilibria," SPE 13951, *SPE Reservoir Engineering*, 1987, v 2, n 4, p 695-702.
- Ammar, M. N. and Renon, H., "The Isothermal Flash Problem: New Methods for Phase Split Calculations," *AIChE J.*, 1987, v 33, n 6, p 926-939.
- Asselineau, L., Bogdanic, G., and Vidal, J.: "A Versatile Algorithm for Calculating Vapour-Liquid Equilibria," *Fluid Phase Equilibria*, 1979, v 3, n 4, p 273-290
- Baker, L. E., Pierce, A. C., and Luks, K. D.: "Gibbs Energy Analysis of Phase Equilibria," SPE 9806, *SPEJ*, 1982, v 22, n 5, p 731-742.
- Bennet, C., Brasket, C. and Tierney, J.: "Calculations of Equilibrium Flash Vaporization Curves by an Integration Method," *AIChE J.*, 1960, v 6, n 1, p 67-70.
- Canjar, L. N. and Manning, F. S.: "Thermodynamic Properties and reduced Correlations for Gases," Gulf Publishing Co., Houston, Texas, 1967.
- Chen, Z.: "Reservoir Simulation: Mathematical Techniques in Oil Recovery, " Society for Industrial and Applied Mathematic (SIAM), Philadelphia, Pennsylvania, 2007.
- CMG-Computer Modeling Group: "WinProp User's Guide – Version 2013", Computer Modeling Group Ltd., Calgary, Alberta, 2014.
- Culberson, O. L. and Mcketta Jr., J. J.: "Phase Equilibria in Hydrocarbon-Water Systems II – The Solubility of Ethane in Water at Pressures to 10,000 psi," *JPT*, 1950, v 2, n 11, p 319-322
- Culberson, O. L. and McKetta Jr., J. J.: "Phase Equilibria in Hydrocarbon-Water Systems III – The Solubility of Methane in Water at Pressures to 10,000 psia," *JPT*, 1951, v 3, n 8, p 223-226.

- Cysewski, G. R. and Prausnitz, J. M.: "Estimation of Gas Solubilities in Polar and Nonpolar Solvents," *Ind. Eng. Chem. Fundamentals*, 1976, v 15, n 4, p 304-309.
- Deam, J. and Maddox, R.: "How to Figure Three-Phase Flash," *Hydrocarbon Processing*, 1969, v 48, n 7, p 163-164.
- Dluziewski, J., Alder, S. and Ozardesh, H.: "Aid to Correlation of Complex Equilibria," *Chem. Eng. Prog.*, 1973, v 69, n 11, p 79-80
- Enick, R. M., Holder, G. D., Grenko, J. A. and Brainard, A. J.: "Four-Phase Flash Equilibrium Calculations for Multicomponent Systems Containing Water," *ACS Symposium Series*, 1986, v 300, p 494-518.
- Enick, R. M., Holder, G. D., Mohamed, R.: "Four-Phase Flash Equilibrium Calculations Using the Peng-Robinson Equation of State and a Mixing Rule for Asymmetric Systems," *SPE Reservoir Engineering*, 1987, v 2, n 4, p 687-694.
- Erbar, J. H.: "Thermodynamic Property Predictions in Process Design," Proc., Symposium on Vapor-Liquid Equilibria in Multicomponent Mixtures, Jablonna, Poland, Nov. 3-6, 1972.
- Erbar, J. H., Jagota, A. K., Muthswamy, S. and Moshfeghian, M.: "Predicting Synthetic Gas and Natural Gas Thermodynamic Properties Using a Modified Soave-Redlich-Kwong Equation of State," Research Report RR-42, Gas Processors Association, Tulsa, OK, Aug, 1980.
- Evelein, K. A., Moore, R. G. and Heidemann, R. A.: "Correlation of the Phase Behavior in the Systems Hydrogen Sulfide – Water and Carbon Dioxide – Water," *Ind. Eng. Chem., Process Des. Dev.*, 1976, v 15, n 3, p 423-428.
- Firoozabadi, A.: "Thermodynamics and Applications in Hydrocarbon Energy Production," McGraw-Hill Education, New York City, New York, 2016

- Fussell, D. D. and Yanosik, J. L.: "An Iterative Sequence for Phase-Equilibria Calculations Incorporating the Redlich-Kwong Equation of State," *SPEJ*, 1978, v 18, n 3, p 173-182.
- Fussell, L.: "A Technique for Calculating Multiphase Equilibria," SPE 6722, *SPEJ.*, 1979, v 19, n 4, p 203-210.
- Gautam, R. and Seider, W. D.: "Computation of Phase and Chemical Equilibrium. Part I. Local and Constrained Minima in Gibbs Free Energy," *AIChE J.*, 1979, v 25, n 6, p 991-999.
- Heidemann, R. A.: "Three-Phase Equilibria Using Equations of State," *AIChE J.*, 1974, v 20, n 50, p 847-855.
- Heidemann, R. A. and Prausnitz, J. M.: "Equilibrium Data for Wet-Air Oxidation, Water Content and Thermodynamic Properties of Saturated Combustion Gases," *Ind. Eng. Chem. Process Des. Dev.*, 1977, v 16, n 3, p 375-381
- Huang, E. T. S. and Tracht, J. H.: "The Displacement of Residual Oil by Carbon Dioxide," SPE 4735, presented at the SPE Improved Oil Recovery Symposium, Tulsa, Oklahoma, Apr 22-24, 1974.
- Jonah, D. A.: "A New Correlation for Henry's Constant for the Solubility of Gases and Liquids", *Fluid Phase Equilibria*, 1983, v 15, n 2, p 173-187
- Khan, S. A., Pope, G. A., and Sepehrnoori, K.: "Fluid Characterization of Three-Phase CO₂/Oil Mixture," SPE 24130, presented at the SPE/DOE Enhanced Oil Recovery Symposium, Tulsa, Oklahoma, Apr 22-24, 1992.
- Kobayashi, R. and Katz, D. L.: "Vapor-Liquid Equilibria for Binary Hydrocarbon-Water Systems," *Ind. Eng. Chem.*, 1953, v 45, n 2, p 440-446.
- Li, Y. and Nghiem L. X.: "Phase Equilibria of Oil, Gas and Water/Brine Mixtures from a Cubic Equation of State and Henry's Law," *Can. J. of Chem. Eng.*, 1986, v 64, n 3, p 486-496.

- Li, Z. and Firoozabadi, A.: "General Strategy for Stability Testing and Phase-split Calculation in two and three phases," *SPEJ*, 2012, v 17, n 4, p 1096-1106.
- Litvak, M. L.: "New Procedure for Phase-Equilibrium Computations in Compositional Reservoir Simulators," *SPE Adv. Tech. Series*, 1994, v 2, n 2, p 113-121.
- Lu, B., Yu, P. and Sugie, A.: "Prediction of Vapor-Liquid-Liquid Equilibria by Means of a Modified Regula-Falsi Method," *Chem. Eng. Sci.*, 1974, v 29, n 2, p 321-326.
- Lucia, A., Miller, D. C. and Kumar, A.: "Thermodynamically Consistent Quasi-Newton Formulae," *AIChE J.*, 1985, v 31, n 8, p 1381-1388.
- Luks, K. D., Fitzgibbon, P. D., and Banchemo, J. T.: "Correlations of the Equilibrium Moisture Content of Air and of Mixtures of Oxygen and Nitrogen for Temperatures in the Range of 230 to 600K at pressure up to 100 Atm," *Ind. Eng. Chem. Process Des. Dev.*, 1976, V 15, n 2, p 326-332.
- Lyckman, E. W., Eckert, C. A. and Prausnitz, J. M.: "Generalized reference Fugacities for Phase Equilibrium Thermodynamics," *Chem. Eng. Sci.*, 1965, v 20, n 7, p 685-691
- Mehra, R. K., Heidemann, R. A. and Aziz, K.: "Computation of Multiphase equilibrium for Compositional Simulation," *SPEJ*, 1982, v 22, n 1, p 61-68.
- Mehra, R. K., Heidemann, R. A. and Aziz, K.: "An Accelerated Successive Substitution Algorithm," *Can. J. of Chem. Eng.*, 1983, v 61, n 4, p 590-596.
- Metcalf, R. S. and Yarborough, L.: "The Effect of Phase Equilibria on the CO₂ Displacement Mechanism," SPE 7061, *SPEJ*, 1979, v 19, n 4, p 242-252.
- Michelsen, M. L.: "The Isothermal Flash Problem. Part I. Stability," *Fluid Phase Equilibria*, 1982a, v 9, n 1, p 1-19.

- Michelsen, M. L.: "The Isothermal Flash Problem. Part II. Phase-split Calculation," *Fluid Phase Equilibria*, 1982b, v 9, n 1, p 21-40.
- Nghiem, L. X., and Heidemann, R. A.: "General Acceleration Procedure for Multiphase Flash Calculation with Application to Oil-gas-water Systems," *Proc.*, 2nd Eur. Symposium on Enhanced Oil Recovery, Nov 8-10, 1982, Paris, Editions Technip, Paris, p 303-316.
- Nghiem, L. X.: "A New Approach to Quasi-Newton Methods with Application to Compositional Modeling", SPE-12242, presented at SPE Reservoir Simulation Symposium, San Francisco, California, Nov 15-18, 1983.
- Nghiem, L. X., Aziz, K. and Li, Y.: "A Robust Iterative Method for Flash Calculations Using the Soave-Redlich-Kwong or the Peng-Robinson Equation of State", SPE 8285, *SPEJ*, 1983, v 23, n 3, p 521-530.
- Nghiem, L. X. and Li Y.: "Computation of Multiphase Equilibrium Phenomena with an Equation of State", *Fluid Phase Equilibria*, 1984, v 17, n 1, p 77-95.
- Nghiem, L. X. and Li Y.: "Effect of Phase Behavior on CO₂ Displacement Efficiency at Low Temperatures: Model Studies with an Equation of State", SPE 13116, *SPE Reservoir Engineering*, 1986, v 1, n 4, p 414-422.
- Ohanomah, M. O. and Thompson, D. W.: "Computation of Multicomponent Phase Equilibria – Part I. Vapor-Liquid Equilibria," *Comp. & Chem. Eng.*, 1984, v 8, n 3, pp 147-156.
- Okuno, R.: "Modeling of Multiphase Behavior for Gas Flooding Simulation," Ph.D. Dissertation, the University of Texas at Austin, 2009.
- Olds, R. H., Sage, B. H. and Lacey, W. N.: "Phase Equilibria in Hydrocarbon Systems," *Ind. Eng. Chem.*, 1942, v 34, n 10, p 1223-1227.

- Organick, E. and Meyer, H.: "Flash Calculations as Performed on the IBM Card Programmed Calculator," *JPT*, 1955, v 7, n 5, p 9-13.
- Orr Jr., F. M. and Jensen C. M.: "Interpretation of Pressure-Composition Phase Diagrams for CO₂/Crude-Oil Systems," SPE 11125, *SPEJ*, 1984, v 24, n 5, p 485-497.
- Osborne, A.: "How to Calculate Three-phase Vaporization," *Chem. Eng.*, 1964, v 71, n 25, p 97-98
- Peneloux, A., Rauzy, E. and Freze, R.: "A Consistent Correction for Redlich-Kwong-Soave Volumes", *Fluid Phase Equilibria*, 1982, v 8, n 1, p 7-23.
- Peng, D. Y. and Robinson, D. B.: "A New Two-Constant Equation of State," *Ind. Eng. Chem. Fund.*, 1976a, v. 15, n 1, p 59-64.
- Peng, D. Y. and Robinson, D. B.: "Two and Three Phase Equilibrium Calculations for Systems Containing Water," *Can. J. of Chem. Eng.*, 1976b, v 54, n 6, p 595-599.
- Peng, D. Y. and Robinson, D. B.: "Two- and Three-Phase Equilibrium Calculations for Coal Gasification and Related Processes," *Thermodynamics of Aqueous Systems with Industrial Application*, 1980, Newman, S. A., Ed. Amer. Chem. Soc. Symp. Ser, 133, p 393-414.
- Prausnitz, J. M.: "Molecular Thermodynamics of Fluid Phase Equilibria," Prentice-Hall, Englewood Cliffs, New Jersey, 1969.
- Prausnitz, J. M., Anderson, T. F., Grens, E.A., Eckert, C.A., Hsieh, R. and O'Connell, J.P.: "Computer Calculations for Multicomponent Vapour-Liquid and Liquid-Liquid Equilibria," Prentice-Hall, Englewood Cliffs, New Jersey, 1980.
- Rachford, H. H. and Rice, J. D.: "Procedure for Use of Electronic Digital Computers in Calculating Flash Vaporization Hydrocarbon," *JPT*, 1952, v. 4, n. 10, p 19-20.

- Reamer, H. H., Olds, R. H., Sage, B. H. and Lacey, W. N.: "Phase Equilibria in Hydrocarbon Systems. Composition of Dew-Point Gas in Ethane-Water System," *Ind. Eng. Chem.*, 1943, v 35, n 7, p 790-793.
- Reid, R. C., Prausnitz, J. M. and Sherwood T. K.: "The Properties of Gases and Liquids, Third Edition," 1977, McGraw-Hill, New York City, New York, 1977.
- Risnes, R. and Dalen, V.: "Equilibrium Calculation for Coexisting Liquid Phases," SPE 11126, *SPEJ*, 1984, v 24, n 1, p 87-95.
- Rowe, A. M. and Chou J. C. S.: "Pressure-Volume-Temperature-Concentration relation of Aqueous NaCl Solutions," *J. Chem. Eng. Data*, 1970, v 15, n 1, p 61-66
- Shelton, J.L. and Yarborough L.: "Multiple Phase Behavior in Porous Media during CO₂ or Rich-Gas Flooding," SPE 5827, *JPT*, 1977, v 29, n 9, p 1171-1178.
- Soave, G.: "Equilibrium Constants from a Modified Redlich-Kwong Equation of State," *Chem. Eng. Sci.*, 1972, v 27, n 6, June, p 1197-1203.
- Teh, Y. S. and Rangaiah, G. P.: "A Study of Equation-Solving and Gibbs Free Energy Minimization Methods for Phase Equilibrium Calculations," *Chem. Eng. Res. & Des.*, 2002, v 80, n 7, p 745-759.
- Trangenstein, J. A.: "Minimization of Gibbs Free Energy in Compositional Reservoir Simulation," SPE 13520, presented at SPE Reservoir Simulation Symposium, Dallas, Texas, Feb 10-13, 1985.
- Turek, E. A., Metcalfs, R. S., Yarborough, L. and Robinson Jr., R. L.: "Phase Equilibria in CO₂ - Multicomponent Hydrocarbon Systems: Experimental Data and an Improved Prediction Technique," SPE 9231, *SPEJ*, 1984, v 24, n 3, p 308-324.

Wei, Y.: “Development of a Four-Phase Compositional Simulator using Equations of State,” Ph.D. Dissertation, the University of Calgary, 2015.

Wiebe, R.: “The Binary System Carbon Dioxide-Water under Pressure,” *Chemical Reviews*, 1941, v 29, n 3, p475-481

Wilson, G.G.: “A modified Redlich-Kwong Equation of State, Application to General Physical Data Calculations,” presented at the AIChE 65th National Meeting, Cleveland, OH, May 4-7, 1969.

Yen, L. C. and Alexander R. E.: “Estimation of Vapor and Liquid Enthalpies,” *AICHE J.*, 1965, v 11, n 2, p 334-339